EXPERIMENTAL VALIDATION OF SHUT-DOWN DOSE RATES

FINAL REPORT

P. Batistoni, M. Angelone, L. Petrizzi, M. Pillon (1)
H. Freiesleben, D. Richter, K. Seidel, S. Unholzer (2)
Y. Chen, U. Fischer (3)

(1) Associazione Euratom-ENEA sulla Fusione, Via E. Fermi, 44, I-00044 Frascati, Italy
(2) Technische Universität Dresden, Institut für Kern- und Teilchenphysik, Mommsenstrasse 13, D-01062 Dresden, Germany
(3) Association FZK-Euratom, Forschungszentrum Karlsruhe, Institut für Reaktorsicherheit, P.O. Box 3640, D-76021 Karlsruhe, Germany

Reference: ITER TASK T-426

June 2001

INDEX

EXECUTIVE SUMMARY

A neutron irradiation experiment has been performed using the Frascati Neutron Generator (FNG) and a material assembly suitable to generate a neutron flux spectrum similar to that anticipated for the outer vacuum vessel region of ITER. The mock-up was irradiated for a sufficiently long time to create a level of activation which was, after shut down, monitored by dosimeters and other radiation detectors for a cooling time period assumed to be required for allowing personal access.

The experiment configuration was designed to allow the validation of present dose rate calculations in a typical and complex shield geometry, compatible with the intensity of the available neutron source and its capability to induce sufficiently high dose levels in the mock-up.

During May 8-10, 2000, the mock-up was irradiated by 14 MeV neutrons at FNG, in a first campaign for a total of 18 hours in three days. The total neutron production was 1.815×10^{15}. The following measurements were carried out by the ENEA team starting immediately after the irradiation up to the end of July, 2000:

- Dose rate measurements by a Geiger-Müller detector (G-M),
- Gamma-ray dose distribution by TLD,
- Measurement of the Ni-58(n,p)Co-58 and Ni-57(n,2n)Ni-57 reaction rates during irradiation by Ni activation foils.

The assembly was irradiated again during a second experimental campaign at FNG form August 29-30, for a total of 13 hours in two days. A total of 1.95×10^{15} neutrons were produced. The following measurements were carried out by the TUD team starting immediately after the irradiation up to September 21, 2000:

- Dose rate measurements by a tissue-equivalent scintillator,
- Decay gamma-ray flux spectra by a NE 213 scintillator,
- Neutron flux spectrum during irradiation with NE 213 spectrometer.

The experiment was analysed with two different computational approaches:

(1) a rigorous two-step (R2S) method making use of the MCNP transport code and the FISPACT inventory code linked through a suitable coupling scheme for the automated routing of neutron flux spectra and decay gamma sources. This system has been developed as part of Task T-426 on the experimental validation of shut-down dose rates.

(2) a direct one-step method (D1S) with an *ad hoc* modified version of MCNP where neutron and decay gamma transport are handled in one single Monte Carlo calculation run. This approach has been developed with the ITER JCT and is being used for nuclear design analyses of ITER.

In either approach, cross-section data from the FENDL/MC-2 (Monte Carlo transport) and FENDL/A-2 (activation) were used.

The analyses of the experiment showed that:

- The dose rates measured by the two independent methods agree within ±15% with R2S calculations using FENDL/A-2.0 cross-sections. There is a tendency for underestimating the dose rate at short decay times ($\leq \cong$ 2 days) which can be addressed to Mn-56 and Ni-57. This tendency is enhanced for the D1S method in which minor nuclides, contributing to the total dose rate at the percent level, are not considered. At larger cooling times, the dose rate is slightly overestimated. This is likely due to the Co-58 production cross-section in FEND/A-2.0.

- The measured decay gamma-ray spectra can be reproduced rather well by the calculations. The resolution of the calculated peaks in the spectra, however, depends on the way the underlying decay gamma-rays are represented in the calculation. The D1S calculation makes use of discrete lines while the R2S method employs the 24-group structure as provided by FISPACT. Discrete decay gamma-ray emission spectra, however, may be applied in the R2S calculation as well.

- The measured decay gamma-ray flux for energies above 0.4 MeV can be calculated with deviations between -20% and +8% when using FENDL/A-2.0 cross-sections. As with the dose rate, there is a tendency for underestimating the measurements, in particular in the time range 1 to 5 days after irradiation. Again this underestimation is larger for the D1S method than it is for the R2S method.

- In the analysis of the measurement of dose rate distribution by TLDs, good agreement with the experimental data is found with both the R2S and the D1S method for almost all positions. The total experimental uncertainties, however, are rather large. The global features of the dose rate distribution inside the cavity are satisfactorily predicted by the calculations. However, a trend of overestimation is observed at decay times $\geq$ 15 days, consistent with the results of the dose rates in the cavity centre.

- For the Ni-58(n,p)Co-58 activation measurements the R2S method with FENDL/A-2.0 data gives C/E values slightly higher than unity, while the C/E values obtained with the D1S method using IRDF-90 and FENDL/MC–2.0 data are in better agreement with the measurements. For the Ni-58(n,2n)Ni-57 reaction, both methods give C/E values slightly lower than unity; the underestimation being more pronounced by D1S. These results are consistent with those found in the analysis of the dose rates by the R2S and D1S methods.

- The neutron flux spectrum measured in the centre of the cavity during irradiation is well reproduced by a MCNP calculation with FENDL/MC-2.0 data. It provides an independent confirmation of the neutron source monitoring and the normalisation applied to the experimental data.

1. INTRODUCTION

Neutronics experiments are important to validate neutronics design calculations for ITER which rely on codes and nuclear data with inherent uncertainties. Experimental validation is, in particular, required for responses which affect the feasibility and economics of machine components and systems, and which are safety relevant. Within the latter category of problems, present dose rate calculations for complex geometry's suffer from uncertainties which are unacceptable for guaranteeing occupational safety during hands-on maintenance inside the cryostat. Therefore, a neutronics experiment has been performed using the 14 MeV Frascati Neutron Generator (FNG) and a material assembly suitable to generate a neutron flux spectrum similar to that anticipated for the outer vacuum vessel region of ITER. The mock-up was irradiated for a sufficiently long time to create a level of activation which was, after shut down, monitored by dosimeters and other radiation detectors for a cooling time period assumed to be required for allowing personal access. The experiment was analysed (1) with a rigorous two-step (R2S) method [1] which makes use of the MCNP transport code [2] and the FISPACT inventory code [3] linked through a suitable coupling scheme for the automated routing of neutron flux spectra and decay gamma sources, and (2) with a direct one-step method (D1S) [4] using an *ad hoc* modified version of MCNP where neutron and decay gamma transport are handled in one single Monte Carlo calculation run. In either approach, cross-section data from the FENDL/MC-2.0 (Monte Carlo transport) [5] and FENDL/A-2.0 (activation) [6] were used.

2. EXPERIMENT

2.1 Experiment set-up

The configuration was designed to allow the validation of present dose rate calculations in a typical and complex shield geometry, compatible with the intensity of the available neutron source and its capability to induce sufficiently high dose levels in the shield mock-up.

The experimental assembly consisted of a block of stainless steel and water-equivalent material with total thickness of 714 mm, and a lateral size of 1000 mm x 1000 mm (Fig. 1). A cavity was arranged within the block (126.0 mm in the beam direction, 119.8 mm high) behind a 224.7-mm-thick shield. A void channel (27.0 mm inner diameter) was included in front of the cavity to study the effect of streaming paths in the bulk shield (Fig.2). A parallelepiped box was used to locate detectors inside the cavity, with 2-mm-thick bottom and lateral walls (stainless steel AISI316). The assembly was exposed to 14-MeV neutrons generated by FNG. Measurements were taken in the cavity, during the irradiation and after shut-down, to obtain the local neutron flux, the decay gamma-ray spectra and the dose rates for cooling times of interest for maintenance and repair purposes (i.e., about 2 weeks at least).

The assembly was similar to those used for the Bulk Shield Experiment (Task T.218) and for the Streaming Experiment (Task T.362), but modified in order to obtain sufficient dose rate after irradiation. The stainless steel plates were re-arranged in order to have, close to the dose measurement positions (i.e. the cavity),

plates which were less exposed to neutron flux in previous experiments hence with lower residual activation. Plate n. 15 around the cavity is new. The plate order, starting from the surface in front of FNG, as well as their dimensions, are given in Table 1.

Table 1: Dimensions of the mock-up plates, given in the order starting from the neutron source (Fig. 2).

Material / plate n.	**Thickness (mm)**	**Lateral size**
Stainless steel / plate 11	43.5	1000 x 1000 mm^2
12	46.5	”
6	46.5	”
2	46.0	”
15-new	77.0	”
3	49.0	”
1	41.7	”
14	49.5	”
13	48.0	”
10	48.0	”
8	49.0	”
7	50.0	”
Perspex plates / all	20.6	”

The chemical composition of the materials employed in the mock-up is specified in the following:

Stainless steel (SS316) for all layers except n.15 - It is a AISI 316 type steel; the density is 7.954 g/cm^3. The chemical composition, guaranteed by the furnisher and also confirmed by analysis made in ENEA laboratory, is (%w): 68.32 Fe, 16.8 Cr, 10.7 Ni, 2.12 Mo, 1.14 Mn, 0.45 Si, 0.09 Cu, 0.14 Co, 0.16 V, 0.04 C, <0.006 S, 0.022 P, 0.004 Sn, 0.001 Pb, 0.0035 B.

Stainless steel (SS316) for layer n.15 - It is a AISI 316 type steel; the density is 7.954 g/cm^3. The chemical composition, guaranteed by the furnisher and also confirmed by analysis made in ENEA laboratory, is (%w): 66.22 Fe, 17.8 Cr, 11.3 Ni, 2.00 Mo, 1.64 Mn, 0.69 Si, 0.09 Cu, < 0.01 Nb, 0.07 Co, 0.12 V, 0.03 C, < 0.01 S, 0.021 P, < 0.01 Sn, < 0.01 Pb, 0.005 B, < 0.01 Ti, < 0.03 Zr, < 0.01 As, < 0.03 Al.

Stainless steel (SS316) for box - It is a AISI 316 type steel; the density is 7.954 g/cm^3. The chemical composition, guaranteed by the furnisher and also confirmed by analysis made in ENEA laboratory, is (%w): 68.102 Fe, 17.2 Cr, 9.9 Ni, 2.07 Mo, 1.58 Mn, 0.49 Si, 0.42 Cu, 0.011 Nb, 0.10 Co, 0.04 V, 0.023 C, < 0.01 S, 0.039 P, 0.016 Sn, < 0.01 Pb, 0.002 B, < 0.005 Ti, < 0.03 Zr, < 0.01 As, < 0.03 Al.

Perspex (Polymethylmetacrilate) - The composition is $(C_5O_2H_8)_n$ and the density is 1.18 g/cm^3. A sample of this material has been tested in ENEA laboratories and turned out to be of a high degree of purity (Si, S $\approx$ 4 appm; Ca $\approx$ 2.6 appm; Mg, Ti, Fe, K, Na, Al < 1 appm).

2.2 Experimental campaigns

Two experimental campaigns were performed :

1. From May 8-10, 2000 the mock-up was irradiated by 14-MeV neutrons at FNG, for a total of 18 hours in three days (Fig. 3). The total neutron production was 1.815×10^{15}.

The following measurements were carried out in the cavity by ENEA team starting immediately after the irradiation up to the end of July, 2000:

- Dose rate by Geiger-Müller detector.
- Gamma-ray dose distribution by thermoluminescent detectors (TLD).
- Ni-58(n,p)Co-58 and Ni-58(n,2n)Ni-57 reaction rates during irradiation by Ni activation foils.

2. The assembly was irradiated again during a second experimental campaign at FNG from August 29-30, for a total of 13 hours in two days. The total neutron production was at 1.95×10^{15}. Fig. 4 shows the time profile as measured during this irradiation campaign. For use in the activation calculations, the measured time profile of the neutron production was averaged over 5 irradiation and 3 beam-off intervals (see Fig. 4). The effect of this simplified profile on the activity inventories is less than 1% for the considered decay times. Table 2 shows the resulting numerical data of the irradiation history as used in the activation calculations.

The following measurements were carried out by the TUD team starting immediately after the irradiation up to September 21, 2000:

- Dose rate by a tissue-equivalent scintillator.
- Decay gamma flux spectra by a NE 213 scintillator.
- Neutron flux spectrum during irradiation with a NE 213 spectrometer.

Table 2: Irradiation history of the second irradiation campaign as processed for use in the activation calculations.

t_{beg} (s)	t_{end} (s)	Δt_{irr} (s)	Source neutrons
0	17480	17480	$5.31 \times 10^{+14}$
17480	25300	7820	$3.35 \times 10^{+14}$
25300	79440	54140	0.
79440	101580	22140	$9.50 \times 10^{+14}$
101580	102480	900	0.
102480	106300	3820	$1.29 \times 10^{+14}$
106300	106720	420	0.
106720	106860	140	$4.00 \times 10^{+12}$
	Total:	106860	$1.95 \times 10^{+15}$

2.3 Measurements in the first experimental campaign

Before the first irradiation in May, the background dose rate level was accurately measured for one week inside the block cavity: a very steady value of 1.77 cps (± 3.5%) corresponding to 0.33 μSv/h, was found using the Geiger-Müller detector (G-M) used also in the following measurements. A statistical check of the measured data was performed showing that the data followed a gaussian distribution, that indicates that no spurious signals were detected by the counting system. Background measurements were also carried out using the two different types of TLDs, TLD-300 and GR-200, also used in the experiment measurements, and by means of a scintillation detector (SCINTOMAT). The measured background values agreed within the quoted errors (Table 3) although it ought to be stressed that the scintillator had a very large volume and it filled almost the whole cavity.

Both the G-M and the TLD detectors were accurately calibrated in the low dose range (down to 0.35 μSv/h for the G-M tube) using Co-60 secondary standard gamma-ray sources of different intensities. In both cases, the calibration errors were < ± 5% even at the lowest dose rate. All calibrations refer to air dose.

Table 3: Comparison among background dose rate measurements

Detector	BKG (μSv/h)	Error
G-M Tube	0.33	± 6%
TLD-300	0.32	± 12%
GR-200	0.32	± 12%
SCINTOMAT	0.38	± 10%

The shut-down dose rate was measured by a Geiger-Müller detector (Mod. 7312 from Vacutec Company) and a Multi-Channel Scaler (MCS) with variable dwell time (from EG&G Ortec company). The size of the detector is 12 mm in diameter, 80 mm in length. Measurements by G-M tube were taken in the centre of the cavity (Fig. 2), in front of the open channel, starting just after the FNG shut-down to obtain the dose rate versus time from half an hour to more than two months of cooling time. The total experimental uncertainty was ± 10% for G-M detector. The quoted error accounts for several contributions (summed by quadratic law): statistics and background (<±5%), calibration (<±5%), dead time (<±2%), energy dependence of the G-M response (±5%) and angular dependence of the G-M response (±5%). The latter contribution was directly measured by locating the G-M tube in the cavity and rotating its orientation of 90°. It was found that the measured count rate was unchanged within ±5%. The total error quoted for G-M tube is almost constant from the highest down to the lowest detectable dose rate. This is possible thanks to the possibility to increase the dwell time used for collecting the data in order to keep as constant as possible the counting statistical uncertainty (<±3%). The G-M tube was also calibrated at high count rate to allow its use just after shut-down, when the expected dose rate level is above the linear response range of the detector. The calibration was performed by measuring the counting rate as a function of different high dose emission rates and then fitting the non linear curve by means of an

exponential function. This exponential behaviour is expected from theory as G-M tubes are paralysed systems when working at high count rate.

Since from activation calculation it is expected that immediately after shut down about 99% of the measured dose is due to Mn-56 decay, a fitting of the dead-time corrected dose rate curve must give the decay constant for such nuclide. Indeed, fitting the dead-time corrected dose rate by a logarithmic function the figure of λ_{exp} = 7.338x10^{-5} s^{-1} is obtained for Mn-56 to be compared with the value of λ = 7.466x10^{-5} s^{-1} used in FENDL/A–2.0. The two data agree better than 2%.

The dose rate in the cavity centre was also measured by high sensitivity thermoluminescent detectors of the type TLD-300 (CaF_2:Tm) from Harshaw Company and Chinese GR-200A (LiF:Mn, Cu, P). The TLDs were chosen, since they allow a complete independent dose rate measurement although they are used just at the limit of their response range. The total error associated with the measurement is ±17%. The contributions to the error come from statistics (between ± 5% and ± 8%), background (± 14%) and calibration (± 5%). Measurements were carried out at four decay times locating four TLDs of each type, enclosed in a polyethylene holder 1-mm thick, close to the G-M dosimeter for time intervals ranging from 18 to 22.5 hours (Table 4). Fig. 5 shows the measured dose rate in the centre of the cavity versus cooling time (after background subtraction), both for G-M and for TLD detectors. The comparison of the results obtained with the two techniques is in agreement within 12%, well within the combined experimental uncertainties.

The dose rate distribution in the cavity was measured at the same times, using the same TLDs located all around the cavity walls (Fig. 2). In each experimental position, four TLDs of each type were located inside a polyethylene holder (1-mm thick). The starting time (referred to the end of irradiation) and duration for each series of measurement is the same as before (see Table 4). Table 5 reports the average values of dose rate measured by using the two different types of TLDs. As the dose rate measured with TLDs is at their sensitivity limit, the used measuring time was a compromise between the need to avoid a too long integration and to have an acceptable integrated dose in the dosimeter.

Table 4: TLD measurements

Measurement	Starting time	Duration	Mean cooling time
1	6.798x10^5 s	18.0 h	7.122x10^5 s
2	1.029x10^6 s	22.5 h	1.069x10^6 s
3	1.621x10^6 s	20.5 h	1.658x10^6 s
4	2.829x10^6 s	21.0 h	2.867x10^6 s

Table 5: Measured dose rate distribution by TLDs along the cavity walls (μSv/h).

Position	Measurem. 1	Measurem. 2	Measurem. 3	Measurem. 4
Cavity centre	0.56	0.50	0.43	0.34
1	0.64	0.58	0.39	0.34
2	0.55	0.51	0.46	0.31
3	0.53	0.52	0.45	0.33
4	0.93	0.77	0.71	0.59
5	0.67	0.55	0.47	0.39
6	0.48	0.45	0.29	0.28

Ni-58(n,p)Co-58 and Ni-58(n,2n)Ni-57 activation reaction rates during irradiation were measured by Ni foils located all around the cavity walls (Fig. 2). The goal was to measure independently the production of Co-58, which is responsible of most of the dose rate in the relevant decay time, and of Ni-57 which is the second most important contributor to total dose rate in the first week after shut-down, when Mn-56 has decayed (see Fig. 7). The total experimental error was ±4.5% and it results from several contributions coming from FNG neutron source uncertainty (± 3%), counting statistics (<±2%) and detector (HPGe) absolute calibration (±2.5%). The experimental results are included in Tables 7 and 8 below.

2.4 Measurements in the second experimental campaign

The shut-down dose rate was measured with a special plastic scintillator (NE 105) having nearly linear energy response. The dimension of the cylindrical detection volume was 46 mm both in height and diameter. The mass density of the material was 1.037 g/cm^3, composed to 52.34 at-% of H and to 47.66 at-% of C.

The calibration of the detector was carried out at Physikalisch-Technische Bundesanstalt Braunschweig in photon fields with energies ranging from 19.9 keV up to 6.7 MeV based on the air-kerma reference value of $(W/e)_{air}$ = 33.97 V. The uncertainty at the reference energy E_γ = 662 keV was 1.5%, taking into account the standard uncertainty of the measurement and multiplied by an extension factor of 2. The weak energy dependence of the measured detector response was fitted in the range of energy relevant for the present experiment, E_γ = 50 keV .... 6.7 MeV, and expressed by a correction factor

$$k(E_\gamma) = 7.328 \cdot 10^{-4} \cdot E_\gamma^3 - 1.416 \cdot 10^{-2} \cdot E_\gamma^2 + 0.1605 \cdot E_\gamma + 0.8997, \quad \text{with } k(662 \text{ keV}) = 1.0.$$

The detector had also some sensitivity to the incidence angle of the gamma-radiation. It was determined by MCNP-FISPACT calculations and resulted, together with the above $k(E_\gamma)$, in correction values (as function of the decay time) ranging between 1.025 and 0.97.

As the measurement was carried out simultaneously with the gamma-flux spectra determination, the detector position (middle point of the scintillator) was

shifted by 27.05 mm downward from the central position of the channel and the box (Fig. 2).

Before starting the second irradiation, a dose rate of 0.518 μSv/h (± 0.001 μSv/h statistical uncertainty) was measured in the cavity. This background level was higher than that before the first irradiation by 0.188 μSv/h. The gamma-flux spectrum of the background measured in the cavity showed that ^{58}Co is the dominant gamma radiation source produced in the first irradiation campaign of May 8-10, 2000. Also ^{54}Mn, ^{60}Co and ^{57}Co significantly contribute to the background dose rate. During the 20 days of the second campaign it decreased slightly to a value of 0.4523 μSv/h at the irradiation end (calculated with FISPACT). The background as a function of the decay time is included in Fig. 13 a.

The measurement of the dose rate was started 73 minutes and finished 20 days after the end of the irradiation. The data acquisition with the dose rate meter mab 500 (Münchener Apparatebau) was quasi-continuous over this period: For a given time interval (5 min at the beginning and 3 h at the end of the campaign) the detector signal was integrated and divided by that time. Immediately at the end of the interval the next was started. Interruptions occurred only, when the interval width was changed. In this way the statistical uncertainties of the measured values could be kept below 1%.

The results of the experiment are presented in Fig. 13 a in the time interval structure of the measurement and in Table 9 below for 19 decay times. The uncertainties of the experimental results of 3.9% include 2.5% of the dose rate values (1.5% and 1.7% for calibration and correction factor k_q, respectively; 1% statistical uncertainty of measurement and background) and 3.0% of the neutron source monitoring.

Flux spectra of the decay gamma-rays were measured with a NE 213 liquid scintillator. The dimensions of the cylindrical active volume were 38 mm both in height and diameter. The material had a mass density of 0.874 g/cm^3 and an elemental composition of 54.8 at-% H and 45.2 at-% C. The scintillator was coupled to a photon multiplier by means of a 500 mm long light guide. In this way the interference with the radiation field inside the cavity was reduced.

The pulse-height response of the detector was determined on the basis of detailed simulations of experimental distributions from mono-energetic gamma-sources with the MCNP-4A code. The DIFBAS code [7] was employed for unfolding the measured pulse-height distributions of the present experiment in order to generate the gamma flux spectra. They were obtained as absolute fluxes, as the response matrix has been determined on an absolute scale.

The measurement of gamma flux spectra was carried out simultaneously with the dose rate measurements. Therefore, the detector position (middle point of the scintillator) was above the central position of the channel and of the box by 25.95 mm (Fig. 2). Spectra obtained at several decay times are presented in Figs. 14a-g.

The background flux spectrum was simultaneously measured with the dose rate background before the irradiation of the assembly. A reasonable effect-to-background ratio was observed at the end of the campaign. For shorter times, the background correction was smaller, or could even be neglected for t = 2.08 h.

The integral of the gamma flux for energies E > 0.4 MeV are given in Table 10 below. Their uncertainties take into account those of the measured flux spectra, the background subtraction and the neutron source monitoring.

The neutron flux spectrum during irradiation was measured with the same detector as used for the measurement of the gamma flux spectra. Neutron and gamma events were distinguished by the pulse shape. The pulse-height response of the detector with respect to neutrons was measured at Physikalisch-Technische Bundesanstalt Braunschweig for mono-energetic neutrons in the energy range from 1 MeV up to 16 MeV and compared with Monte Carlo simulations using the NRESP7 code [8].

The measurement was carried out in the central position of the channel and of the box in a short run before the intense irradiation of the block. The number of source neutrons produced for this flux measurement was $7.5 \cdot 10^{-5}$ of that for the intense activation. The ratio of the corresponding neutron fluxes in the cavity was $8.7 \cdot 10^{-4}$, also showing that activation induced by the neutron flux measurement could be neglected. Nevertheless, after the neutron flux measurement the dose rate in the cavity was determined with the mab 500 device as a function of the decay time up to the beginning of the long and intense irradiation. It confirmed, that no additional background, originating in this flux measurement, had to be taken into account.

The measured flux spectrum is displayed in Fig. 16 together with the result of a MCNP-4B/FENDL-2 calculation. The dominant part at the detector position on the streaming channel axis is the 14-MeV neutron peak. Due to the small number of detector events for neutron energies between E = 4 MeV and E = 13.7 MeV, relatively large statistical fluctuations appear in that region. With respect to material activation by fast neutrons, the flux with E > 13.7 MeV is important, as the peak contains 71% of the neutron flux with E > 1 MeV, and with increasing E more and more reaction channels are open and produce radioactivity.

3. COMPUTATIONAL TOOLS

The experiment was analysed (1) with a rigorous two-step (R2S) method [1] which makes use of the MCNP transport code [2] and the FISPACT inventory code [3] linked through a suitable coupling scheme for the automated routing of neutron flux spectra and decay gamma sources, and (2) with a direct one-step method (D1S) using an *ad hoc* modified version of MCNP [4,9] where neutron and decay gamma transport are handled in one single Monte Carlo calculation run. In either approach, cross-section data from the FENDL/MC-2.0 (Monte Carlo transport) [5] and FENDL/A-2.0 (activation) [6] were used.

3.1 Rigorous, two-step method (R2S)

As part of Task T-426 on the experimental validation of shut-down dose rates a computational scheme for a rigorous calculation of the shutdown dose rate distribution in full three-dimensional geometry has been developed [1]. The scheme is based on the use of MCNP for the transport calculations (neutron and decay photons) and FISPACT for the inventory calculation (decay gamma source). A suitable coupling scheme has been devised to enable an automated routing of the MCNP neutron flux spectrum distributions to FISPACT and the FISPACT decay gamma source distributions to MCNP (Fig. 6). The decay gamma source distribution is sampled in a source routine linked to MCNP according to the distribution provided by the preceding MCNP neutron transport and FISPACT inventory calculations.

Two different MCNP models of the FNG assembly were employed: one for the neutron transport calculation during irradiation (Fig. 7a, “irradiation model”) and the other one for the decay gamma transport calculation after irradiation (Fig. 7 b-d, “shut-down model”). In this way proper account is taken of the fact that during the irradiation the central cavity was empty and the lateral access was plugged whereas after irradiation the plug was removed and the detectors were inserted into the cavity.

In the R2S approach, the neutron flux spectra are calculated in the VITAMIN-J 175 group structure for all non-void cells of the “FNG irradiation model” and are routed to FISPACT through the interface MCFISP. Activation inventories and decay gamma sources (spectrum and intensity) are then calculated for all material cells making use of the associated neutron flux spectra. This requires one FISPACT-calculation per cell and material taking into account the proper irradiation history. The resulting decay gamma source distribution is then routed back to MCNP through the interface FISPMC. The MCNP decay gamma transport calculation is performed with the “FNG shut-down model” making proper use of the decay gamma sources as provided by the preceding FISPACT calculations for all non-void geometry cells.

In the analysis of the dose rate measurements with the NE 105 plastic scintillator, (TUD measurement campaign), the photon-flux-to-dose-rate conversion factors according to ANSI/ANS-6.1.1-1977 [10] were employed to obtain the dose rate on the basis of the photon fluxes calculated with MCNP tally 4 for in the detector with the proper material composition (1.037 g/cm^3, 52.34 at-% of H and to

47.66 at-%). In the analysis of the dose rate measurements of the ENEA measurement campaign (Geiger-Mueller detector), MCNP photon tally f6 was used to obtain the dose rate in air as measured in the experiment. A spherical air cell with a 1-mm-thick Al wall was used for this purpose in the MCNP model (Fig.7b).

3.2 Direct one-step method (D1S)

The direct 1-step (D1S) method [4] assumes that a radioactive nuclide generated during irradiation spontaneously emits the associated decay gammas. Neutron and decay gamma transport then can be treated in one single Monte Carlo calculation run. On the basis of this assumption, a special version of the MCNP code has been developed at ITER JCT making use of ad hoc data libraries in which the cross sections are taken from FENDL-2.0. Both FENDL/MC-2.0 and FENDL/A-2.0 have been used with this method to calculate the production of the relevant radioactive nuclides. Decay gamma spectra and yields are taken from EAF-99 [11]. When calculating the dose rate, adjustment factors have to be applied to account for the proper decay rate of a specific radioactive nuclide at the considered decay times taking into account the actual irradiation history.

In the D1S calculation, the FNG assembly model with inserted detectors and removed plug was employed as it is not possible in this approach to use two different models for the irradiation and the shut-down period.

4. FIRST CAMPAIGN : EXPERIMENT ANALYSIS

4.1 Analysis of dose rate measurement

Fig. 8 shows the contributions of major nuclides to the total contact dose rate, as calculated by FISPACT at the inner cavity wall. Mn-56 dominates at short times (i.e. t<1 d), Ni-57 at around 1 d, and then Co-58 dominates in the time range of practical interest for allowing personal access for maintenance purposes. The nuclei considered in the figure contribute to more than 95% of the total dose rate, as shown in the same figure by the black line.

The experiment analysis has been carried out by

- the R2S method for cooling times in the range from 1 day to 2 months, the results are given in Fig. 9 (∆). The statistical uncertainty in the MCNP calculations is always less than 2%, both in the calculation of neutron fluxes and in that of gamma dose rates.

- the D1S method for the same cooling time (also in Fig.9): the production rate of radioactive nuclides was calculated both using FENDL/A-2.0 (O) and FENDL/MC-2.0 ( ). The statistical uncertainty ranges between 4 and 6%. The nuclides considered are Mn-56, Co-58, Ni-57, Mo-99, Mn-54, Cr-51, Fe-59 and Co-60, Cu-64 (the same as given in Fig 8).

All results are given in Tables 6a and 6b together with C/E (calculation/experiment) ratios. The total uncertainty on the comparison is obtained summing by quadratic law the uncertainty on E (±10%) and that on C (given in the tables), and the uncertainty on the FNG source calibration (±3%).

Table 6a: Comparison between measured (with G-M) and calculated dose rates in the cavity centre.

Decay time		E (Sv/h)	R2S (FENDL/A-2)	
Days	years		C (Sv/h)	C/E
1	2.74E-03	2.46E-06 ± 10%	2.13E-06 ± 3%	0.87 ± 0.09
7	1.92E-02	6.99E-07 ± 10%	7.03E-07 ± 3%	1.01 ± 0.11
15	4.11E-02	4.95E-07 ± 10%	5.38E-07 ± 3%	1.09 ± 0.11
30	8.22E-02	4.16E-07 ± 10%	4.55E-07 ± 3%	1.09 ± 0.11
60	1.64E-01	3.16E-07 ± 10%	3.49E-07 ± 3%	1.10 ± 0.12

Table 6b: Comparison between measured (with G-M) and calculated dose rates in the cavity centre.

Decay time		D1S (FENDL/A-2)		D1S (FENDL/MC-2)	
days	years	C (Sv/h)	C/E	C (Sv/h)	C/E
1	2.74E-03	1.57E-06 ± 6%	0.62 ± 0.07	1.55E-06 ± 5%	0.63 ± 0.07
7	1.92E-02	5.99E-07 ± 4%	0.86 ± 0.09	5.87E-07 ± 5%	0.84 ± 0.08
15	4.11E-02	4.47E-07 ± 4%	0.90 ± 0.10	4.40E-07 ± 5%	0.88 ± 0.09
30	8.22E-02	4.22E-07 ± 5%	1.01 ± 0.11	4.20E-07 ± 5%	1.01 ± 0.11
60	1.64E-01	3.23E-07 ± 4%	1.02 ± 0.11	3.27E-07 ± 5%	1.03 ± 0.11

In the R2S case, an underestimation is found at 1 day (C/E = 0.87). At larger cooling times (7 d – 60 d) the calculated values of the dose rate, although slightly overestimated, are in agreement with the (G-M) measurements within the total uncertainty on the comparison. C/E results are shown in Fig. 10.

The D1S method gives values systematically lower than the R2S method, especially for decay times ≤ 15 days. In part (≈ 5 %) this may be due to the fact that minor radioisotopes, contributing to the total dose rate at the percent level, are not considered in the D1S method. Other diffrences between the two method are due to the treatment of activation cross sections as a function of energy (group-wise in R2S, point-wise in D1S), and in the geometrical modelling: the R2S method correctly takes into account the fact that during the irradiation the central cavity was empty and the lateral access was plugged whereas after irradiation the plug was removed and the detector was inserted into the cavity, while in the D1S calculation, only the shut down model is used.

The comparison between D1S+FENDL/MC-2.0 and D1S+FENDL/A-2.0 shows good agreement within the uncertainty in the calculations.

4.2 Analysis of dose distribution measurements inside the cavity

As in the previous case, the analysis of dose rate distribution measurements by TLD detectors has been carried out with the R2S method (statistical uncertainty ≤3%) and with the D1S method (statistical uncertainty in the range 3% - 8%).

In both cases, the TLD capsules and positions were exactly described in the MCNP model, as shown in Fig. 7c. The calculated dose rates are compared with the measured ones in Figs. 11 a-f, where the experimental data (indicated by black point, with experimental uncertainty) are the average between TL-300 and Gr-200 results.

The comparison of R2S and of D1S methods show a general agreement within ±15%. In comparison with the experimental data, a good agreement is found with both methods for almost all positions within the rather large total uncertainties, and the global features of the dose rate distribution inside the cavity are satisfactorily predicted by calculation. However, a trend to overestimate by calculation is observed at decay times ≥ 15 days, consistently with what is observed in the analysis of the dose rate in the cavity centre.

4.3 Analysis of Ni-58(n,p)Co-58 and Ni-58(n,2n)Ni-57 activation measurements

The neutron flux at the Nickel foils during irradiation was calculated using MCNP, the Ni-58(n,p)Co-58 or Ni-58(n,2n)Ni-57 reaction rates were calculated in two ways:

1. using a procedure similar to the R2S method, i.e. calculating the Ni activation by FISPACT, with neutron fluxes at the activation foils calculated by MCNP, taking the Ni-58(n,p) or (n,2n) cross sections from FENDL/A -2. Statistical errors of the MCNP flux calculations are ≤ ±2.5%.
2. using a procedure similar to the D1S method, i.e. calculating the Ni activation directly in the MCNP run taking the Ni-58(n,p) and (n,2n) cross sections from the dosimetry file IRDF-90.2 and from the transport file FENDL/MC-2. Statistical errors of the reaction rate calculations are ≤ ±2.5%.

All results for the Ni-58(n,p) reaction are given in Table 7. The total errors on C/E is ± 0.05 and include the statistical error of the MCNP calculations and the experimental error of the measurement (±4.5%). Using FISPACT with FENDL/A–2 (R2S), C/E values are in general slightly higher than unity, while the C/E values obtained with direct MCNP calculation (D1S) using the dosimetry file IRDF-90 and FENDL/MC–2 are generally lower and in better agreement with the measurements.

As far as the Ni-58 (n,2n) reaction is concerned, all results are given in Table 8. Using the direct MCNP calculation (D1S) with the dosimetry file IRDF-90 [12] and FENDL/MC–2 C/E values are very close to unity. Using FISPACT with FENDL/A–2 (R2S), C/E are about 1 - 3% lower than in the previous case.

Table 7: Measured and calculated Ni-58(n,p)Co-58 reaction rates (x10^{-24}/source neutron). Foil numbers refer to positions given in Fig. 7c. X is the distance of the foil centre from the channel axis

Foil		Meas.	MCNP +FISPACT		MCNP Calculation		
n	x (cm)	*E*	C (/A-2)	C/E	C (IRDF-90.2)	C (/MC-2)	C/E
1	-0.25	2.15E-5	2.196E-5	1.02	2.099E-5	2.099E-5	0.98
2	3.75	5.19E-6	5.511E-6	1.06	5.447E-6	5.446E-6	1.05
3	7.25	4.13E-6	4.558E-6	1.10	4.022E-6	4.021E-6	0.97
4	3.75	8.48E-6	9.299E-6	1.10	8.637E-6	8.637E-6	1.02
5	-4.25	7.86E-6	8.311E-6	1.06	7.697E-6	7.695E-6	0.98
6	-4.25	5.15E-6	5.345E-6	1.04	4.990E-6	4.899E-6	0.97

Table 8: Measured and calculated Ni-58(n,2n) reaction rates (x10^{-24}/source neutron). Foil numbers refer to positions given in Fig. 7c. X is the distance of the foil centre from channel axis

Foil		Meas.	MCNP +FISPACT		MCNP Calculation		
n.	x (cm)	E	C (/A-2)	C/E	C (IRDF-90.2)	C (/MC-2)	C/E 90.2 – MC2
1	-0.25	2.84E-6	2.597E-6	0.91	2.618E-6	2.653E-6	0.92-0.93
2	3.75	3.94E-7	3.947E-7	1.00	4.029E-7	4.069E-7	1.02-1.03
3	7.25	2.07E-7	1.912E-7	0.92	1.943E-7	1.965E-7	0.94-0.95
4	3.75	4.92E-7	4.991E-7	1.01	5.105E-7	5.158E-7	1.04-1.05
5	-4.25	4.71E-7	4.282E-7	0.91	4.363E-7	4.408E-7	0.93-0.94
6	-4.25	3.64E-7	3.273E-7	0.90	3.339E-7	3.374E-7	0.92-0.93

These results are consistent with those found in the analysis of the dose rate as they confirm an overestimation of the Ni-58(n,p) reaction and an underestimation of the Ni-58 (n,2n) reaction by R2S + FENDL/A–2 method.

5. SECOND CAMPAIGN : EXPERIMENT ANALYSIS

Both the R2S and the D1S computational approach was applied to calculate the shutdown dose rates and the decay gamma flux spectra and compare them to the measurement results. In either case, the MCNP4C code was used with FENDL/MC-2 data for neutron transport calculations and FENDL/A-2 data for the activation calculations. In the R2S–calculations, two different MCNP models of the FNG assembly were employed: one for the neutron transport calculation during irradiation and the other for the decay gamma transport calculation after irradiation. In this way proper account was taken of the fact that during the irradiation the central cavity was empty and the lateral access was plugged whereas after irradiation the plug was removed and the detectors were inserted into the cavity. In the D1S calculation, the FNG assembly model with inserted detectors and removed

plug was employed as it is not possible in this approach to use two different models for the irradiation and the shut-down period.

In the FISPACT-calculations, the irradiation profile shown in Table 2 above was used to obtain the decay gamma source distribution at the end of the irradiation. Decay gamma dose rates and gamma fluxes were calculated with MCNP at the decay times of the corresponding measurements ranging from ≈ 1 h to 20 days after irradiation. The calculations were normalised to the total neutron production of $1.95 \cdot 10^{15}$ generated by FNG in the second irradiation campaign. In the R2S neutron transport calculation, some 88 million source neutron histories were tracked consuming about 1200 CPU minutes on the Linux cluster machine. For the shutdown dose rate calculations 145 decay gamma source cells were considered. Decay gamma transport calculations were performed for a total of 19 cooling times. In either calculation about 172 million decay gamma source histories were tracked consuming about 1000 CPU minutes per calculation run. In the D1S calculation, around 260 million source particles were tracked consuming about 4000 CPU minutes on the Linux cluster.

5.1 Analysis of dose rate measurement

Calculated and measured dose rate results are reproduced in tabular form in Table 9 for the 19 cooling times considered in the experiment. For the measured data, uncertainties are included as described above in section 2.4 whereas for the calculated data, the statistical error of the Monte Carlo calculation is given. Fig. 13a shows a graphical representation of the calculated and measured shutdown dose rates as a function of the cooling time.

Table 9: Dose rates and C/E (calculation/experiment) comparison for the measurements with the tissue-equivalent scintillator.

Decay time [second]	Experiment Dose rate [μSv/h]	R2S Dose rate [μSv/h]	R2S C / E	D1S Dose rate [[μSv/h]	D1S C / E
4380	488. ± 19.	409.6 ± 2.9	0.84 ± 0.03	390±1.01	0.80±0.03
6180	415. ± 16.	357.8 ± 2.6	0.86 ± 0.03	341±0.88	0.82±0.03
7488	375. ± 15.	325.0 ± 2.3	0.87 ± 0.03	310±0.80	0.83±0.03
11580	268. ± 10	240.7 ± 1.7	0.90 ± 0.04	229±0.59	0.85±0.04
17280	173. ± 7.	158.8 ± 1.3	0.92 ± 0.04	150±0.39	0.87±0.05
24480	101. ± 4.	94.25 ± 0.75	0.93 ± 0.04	88.9±0.23	0.88±0.04
34080	50.6 ± 2.0	47.42 ± 0.46	0.94 ± 0.04	44.6±0.12	0.88±0.04
45780	23.0 ± 0.9	21.39 ± 0.21	0.93 ± 0.04	19.9±0.063	0.87±0.03
57240	11.7 ± 0.5	10.71 ± 0.10	0.92 ± 0.04	9.73±0.045	0.83±0.04
72550	5.80 ± 0.23	5.151 ± 0.057	0.89 ± 0.04	4.54±0.038	0.78±0.04
90720	3.56 ± 0.14	3.134 ± 0.038	0.88 ± 0.04	2.66±0.034	0.75±0.03
132000	2.43 ± 0.09	2.214 ± 0.026	0.91 ± 0.04	1.86±0.027	0.76±0.03
212400	1.78 ± 0.07	1.724 ± 0.020	0.97 ± 0.04	1.5±0.018	0.84±0.04
345600	1.22 ± 0.05	1.264 ± 0.013	1.04 ± 0.04	1.16±0.009	0.95±0.04
479300	0.952 ± 0.037	1.016 ± 0.012	1.07 ± 0.04	0.974±0.005	1.02±0.04
708500	0.759 ± 0.030	0.8208 ± 0.0086	1.08 ± 0.04	0.818±0.003	1.08±0.04
1050000	0.667 ± 0.026	0.7115 ± 0.0075	1.07 ± 0.04	0.725±0.003	1.09±0.04
1670000	0.613 ± 0.024	0.6375 ± 0.0068	1.04 ± 0.04	0.655±0.003	1.07±0.04
1710000	0.614 ± 0.024	0.6318 ± 0.0067	1.03 ± 0.04	0.651±0.003	1.06±0.04

As a general trend, there is observed an overall satisfactory agreement over the considered range of cooling times. A more detailed C/E (calculation/ experiment) comparison (Fig. 13b) reveals an underestimation of the measured dose rate at short cooling times (less than ≅ 2 days) by up to 15 % in case of the R2S calculation. The D1S-calculation underestimates the measured dose rate by 20 to 25 %. The dominating dose rate contributions are due to ^{56}Mn (few hours cooling time) and ^{57} Ni (1 – 5 days cooling time). At larger cooling times, the dominant ^{58}Co contribution gives rise to an overestimation of up to 10%.

5.2 Analysis of decay gamma flux spectra measurement

Measured and calculated decay gamma flux spectra are compared in Fig. 14 a through Fig. 14g for cooling times between 2.0 h and 19.3 days. As a general trend, the measured decay gamma ray spectra can be well reproduced by the calculations. There is, however, a distinctive difference between the spectra calculated by the D1S and the R2S method due to different representations of the decay gamma ray emission spectra. The R2S-calculation handles the decay gamma ray spectra in a 24 group structure as provided by the FISPACT code. The D1S procedure, on the other hand, makes use of discrete gamma lines for the decay gamma ray emission spectra of the ad-hoc prepared data library. This results in a rather fine resolution of the gamma ray peaks in the calculated spectra. Note that discrete decay gamma ray emission spectra can be easily introduced into the R2S procedure if there is a need to.

The total decay gamma flux is displayed in Fig.15a as a function of cooling time as calculated by the R2S and the D1S method. In accordance with the dose rate results, the D1S calculation in general gives lower decay gamma fluxes than the R2S calculation does. Fig.15a includes a comparison for the decay gamma flux above 0.4 MeV which has been measure in the experiment. A corresponding C/E comparsion is shown in Fig.15b and Table 10 in graphical and numerical form, respectively.

There is the same trend as for the dose rate, except for the shortest cooling time. The C/E ratio around unity for this time range comes from the overestimation of the low-energy part of the spectrum, whereas the high-energy part is slightly underestimated. The dose rate, however, is dominated by the contribution from the high energy domain.

Table 10: Calculated total decay gamma fluxes for E>0.4 MeV as a function of cooling time

Decay time [second]	Experiment	R2S		D1S	
	ϕ / [$cm^{-2}\cdot s^{-1}$]	ϕ / [$cm^{-2}\cdot s^{-1}$]	C / E	ϕ / [$cm^{-2}\cdot s^{-1}$]	C / E
2.08 h	$(1.30\pm0.06)\cdot10^{4}$	$(1.40\pm0.01)\cdot10^{4}$	1.08±0.05	$(1.33\pm0.004)\cdot10^{4}$	1.02±0.05
15.9 h	523±22	474 ± 5	0.91±0.04	422. ±2.12	0.81±0.04
25.2 h	178±9	142 ± 2	0.80±0.04	119. ±1.61	0.67±0.04
4.00 d	67.6±3.9	55.7 ± 0.6	0.82±0.05	52.2±0.46	0.77±0.05
8.20 d	38.2±2.2	36.6 ± 0.4	0.96±0.06	36.9±0.20	0.97±0.06
12.2 d	33.7±2.3	32.4 ± 0.4	0.96±0.07	32.9±0.18	0.98±0.07
19.3 d	27.3±1.8	29.6 ± 0.4	1.08±0.07	30.0±0.17	1.10±0.08

5.3 Analysis of neutron flux spectrum measurement

The measured and calculated flux spectra are compared in Fig. 16. The dominant part at the detector position on the streaming channel axis is the 14-MeV neutron peak. It contains 71% of the neutron flux with E > 1 MeV, and with increasing E more and more reaction channels are open and produce radioactivity. The measured fluence of neutrons with E > 13.7 MeV, normalised to one source neutron amounts to $(5.91 \pm 0.35)\cdot10^{-5}$. The corresponding calculated value is $(5.96 \pm 0.32)\cdot10^{-5}$, resulting in a ratio of calculated-to-experimental fluence (C/E) of 1.01 ± 0.07. (Total uncertainty for E and statistical one for C).

6. CONCLUSIONS

The analysis of the experiment showed that:

- The dose rates measured agree within ±15% with R2S calculations using FENDL-2/A cross-sections. There is a tendency for underestimating the dose rate at short decay times ($\leq \cong$ 2 days) which can be addressed to Mn-56 and Ni-57. This tendency is enhanced for the D1S method in which minor nuclides, contributing to the total dose rate at the percent level, are not considered. At larger cooling times, the dose rate is slightly overestimated. This is likely due to the Co-58 production cross-section in FENDL/A-2.

- For the Ni-58(n,p)Co-58 activation measurements the R2S method gives C/E values slightly higher than unity, while the C/E values obtained with the D1S method using IRDF-90 and FENDL/MC–2 are in better agreement with the measurements. For the Ni-58(n,2n)Ni-57 reaction, both methods give C/E values slightly lower than unity, the underestimation being more pronounced by D1S. These results are coherent with those found in the analysis of the dose rate by the R2S and D1S methods.

- The measured decay γ-ray spectra can be reproduced rather well by the calculations. The resolution of the calculated decay gamma peaks, however, depends on the way the underlying decay gamma emission spectra are represented in the calculation. The D1S calculation makes use of discrete decay gamma lines while the R2S method employs the 24 group structure as provided by FISPACT. Discrete decay gamma emission spectra, however, may be applied in the R2S calculation as well.

- The decay gamma flux, measured above 0.4 MeV photon energy in the experiment, can be calculated with deviations between -20% and +8% when using FENDL/A-2.0 cross-sections. As with the dose rate, there is a tendency for underestimating the measurements, in particular in the time range 1 to 5 days after irradiation. Again this underestimation is larger for the D1S method than it is for the R2S method.

- The analysis of the dose rate distribution measurements shows a good agreement with experimental data for almost all positions within the rather large total uncertainties, and the global features of the dose rate distribution inside the cavity are satisfactorily predicted by calculation. However, a trend to overestimate by calculation is observed at decay times $\geq$ 15 days, consistently with what is observed in the analysis of the dose rate in the cavity centre. The comparison of R2S and of D1S methods show a general agreement within $\pm$15%.

- The neutron flux spectrum during irradiation measured in the centre of the cavities well reproduced by a MCNP-4B calculation with FENDL/MC-2.0 data. It also confirms neutron source monitoring and normalisation of the experimental data.

REFERENCES

[1] Y. Chen, U. Fischer, H. Tisge-Tamirat, Rigorous MCNP Based Shutdown Dose Rate Calculations: Computational Scheme, Verification Calculations and Applications to ITER, Forschungszentrum Karlsruhe, Interner Bericht IRS-Nr. 2/01 - FUSION Nr. 166, Januar 2001

[2] Judith F. Briesmeister, Ed, "MCNP - A General Monte Carlo N-Particle Transport Code, Version 4B", Los Alamos National Laboratory Report LA-12625-M (1997).

[3] R. A. Forrest, J-Ch. Sublet, “FISPACT-99: User manual”, Report UKAEA FUS 407, December 1998

[4] Valenza, D.," Proposal of Shutdown Dose Estimation Method by Monte Carlo Code", submitted to the Journal of Fusion Technology and Engineering.

[5] H. Wienke and M. Herman, “FENDL/MG-2.0 and FENDL/MC-2.0 The processed cross-section libraries for neutron photon transport calculations” IAEA-NDS-176 Rev. 1, October 1998

[6] A.B. Pashchenko, H. Wienke, J. Kopecky, J.-Ch. Sublet and R.A. Forrest, “FENDL/A-2.0 Neutron Activation Cross Section Data Library for Fusion Applications” IAEA report IAEA-NDS-173, Rev. 1, October 1998

[7] M. Tichy, The DIFBAS Program – Description and User’s Guide, Report Physikalisch-Technische Bundesanstalt Braunschweig, PTB-7.2-193-1, 1993.

[8] S. Guldbakke, H. Klein, A. Meister, J. Pulpan, U. Scheler, M. Tichy, S. Unholzer, Response Matrices of NE312 Scintillation Detectors for Neutrons, Reactor Dosimetry ASTM STP 1228, ed. H. Farrar et al., American Society for Testing Materials, Philadelphia, 1995, p. 310-322.

[9] H. Iida, D. Valenza,R. Plenteda, R.T. Santoro and Juergen Dietz "Radiation Shielding for ITER to Allow for Hands-on Maintenance inside Cryostat, Journal of Nuclear Science and Technology, Supplement 1,pp 235-242 (March 2000)

[10] ANS-6.1.1 Working Group, M. E. Battat (Chairman), "American National Standard Neutron and Gamma-Ray Flux-to-Dose Rate Factors", ANSI/ANS-6.1.1-1977 (N666), American Nuclear Society, LaGrange Park, Illionois (1977)

[11] J.-Ch. Sublet, J. Kopecky and R. A. Forrest, The European Activation File: EAF-99 cross section library, UKAEA FUS 408, Culham,1998.

[12] N. P. Kocherov, P. K. Mc Laughlin, The International Reactor Dosimetry File, IAEA-NDS-141, Rev. 2, Vienna, 1993.

FIGURES

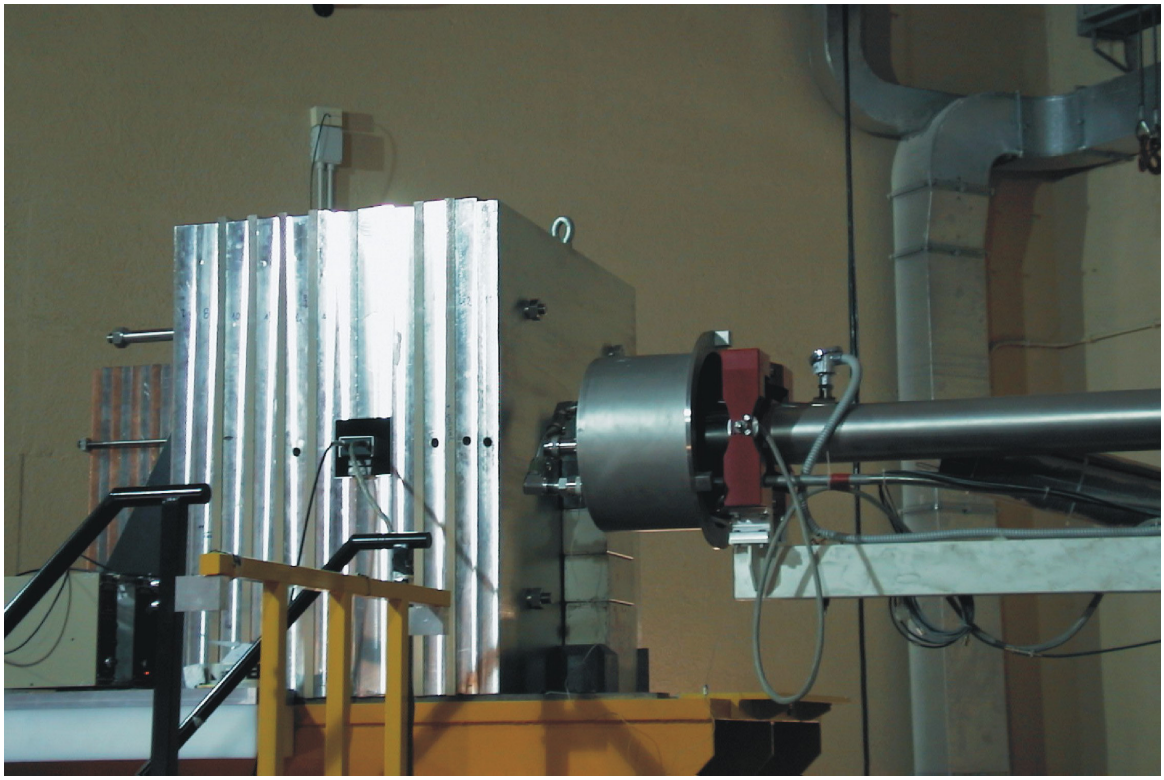

Fig.1: Experimental set-up in front of FNG target

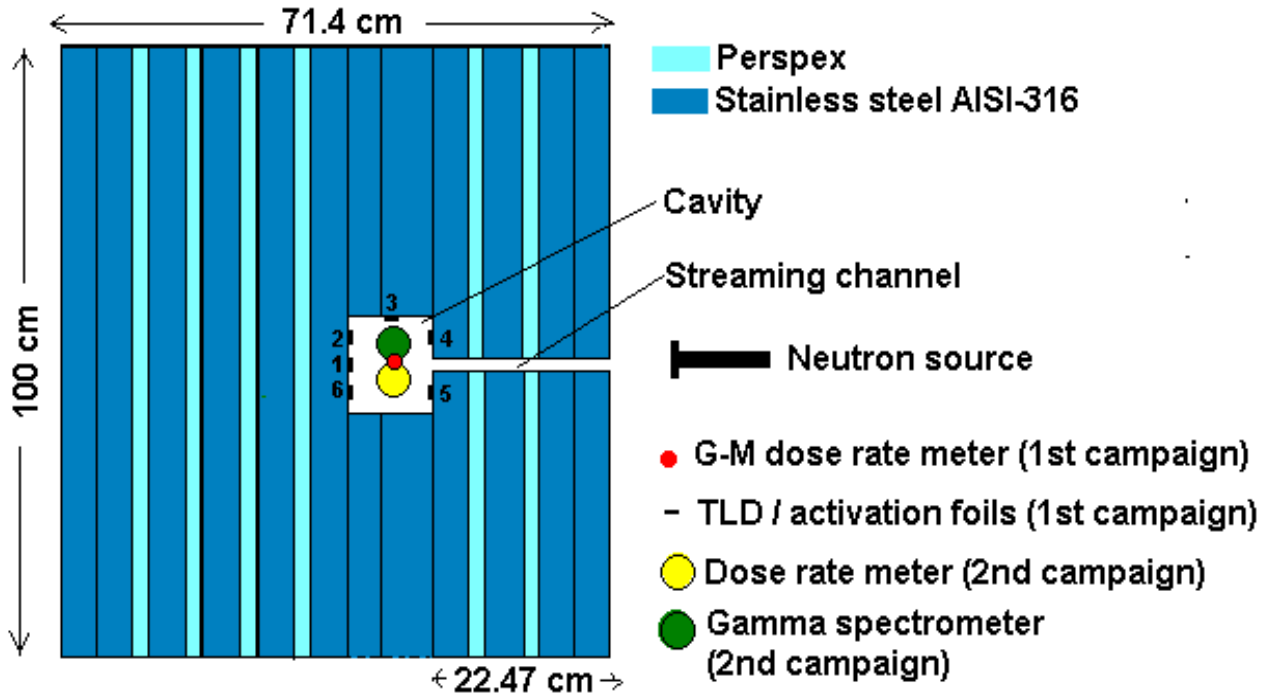

Fig. 2: Schematic view of experimental set-up (vertical section)

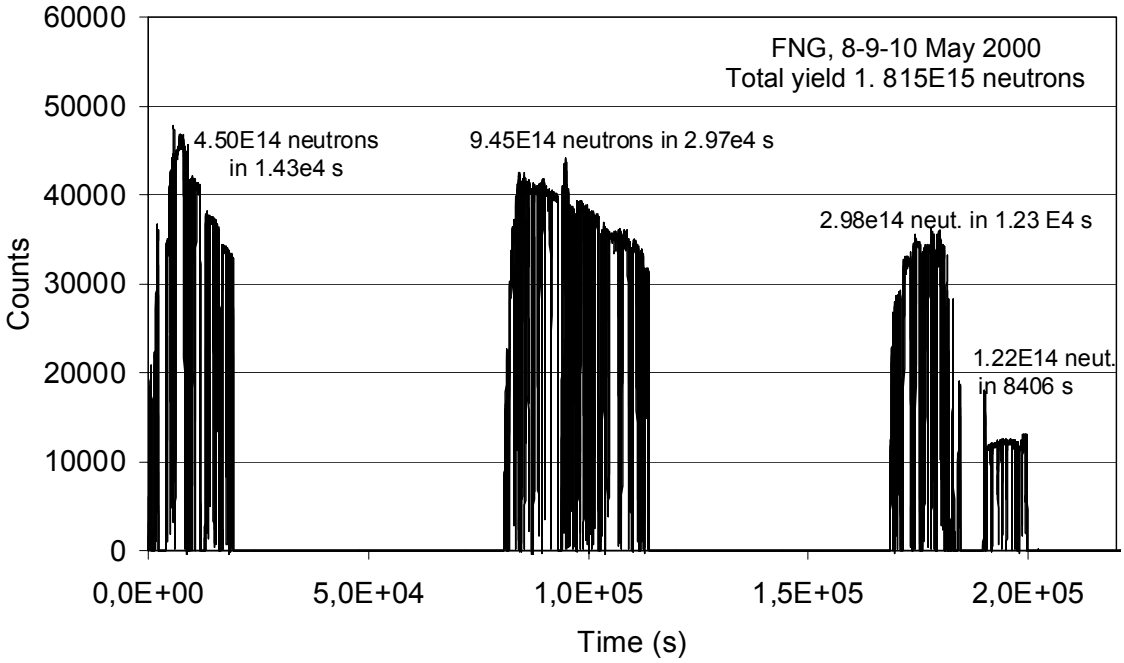

Fig. 3: Time profile of irradiation during the first experimental campaign.

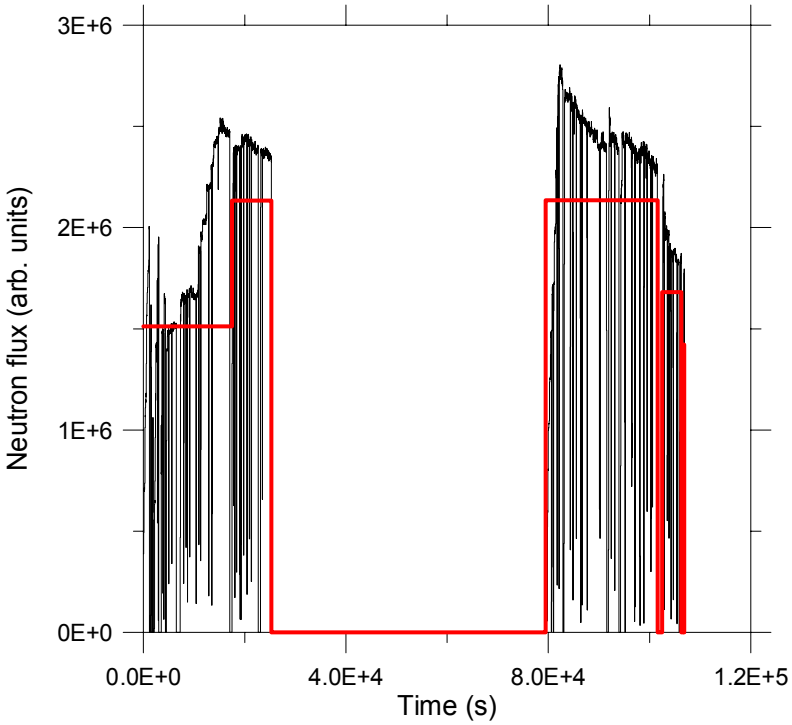

Fig. 4: Time profile of irradiation during the second campaign (thin line) and its representation by the values of Table 2 (red line).

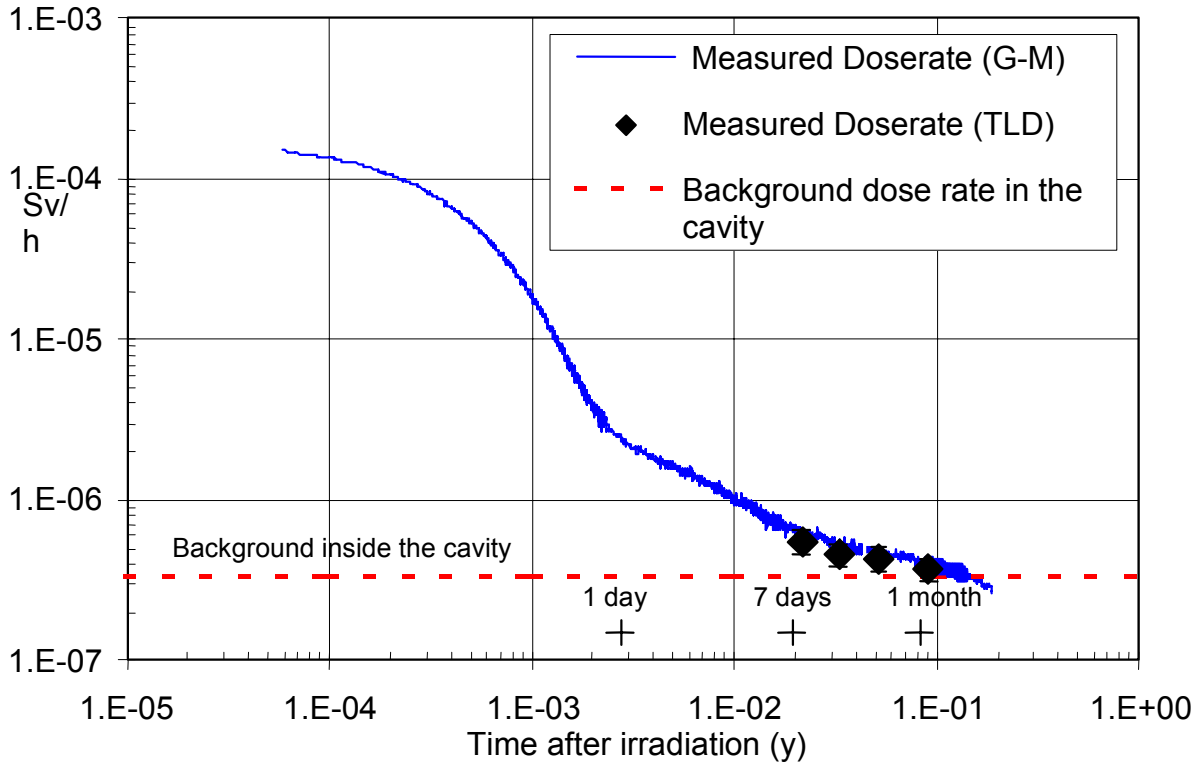

Fig. 5: Measured dose rate inside the cavity versus cooling time (after background subtraction), both for G-M detector and for TLD detectors.

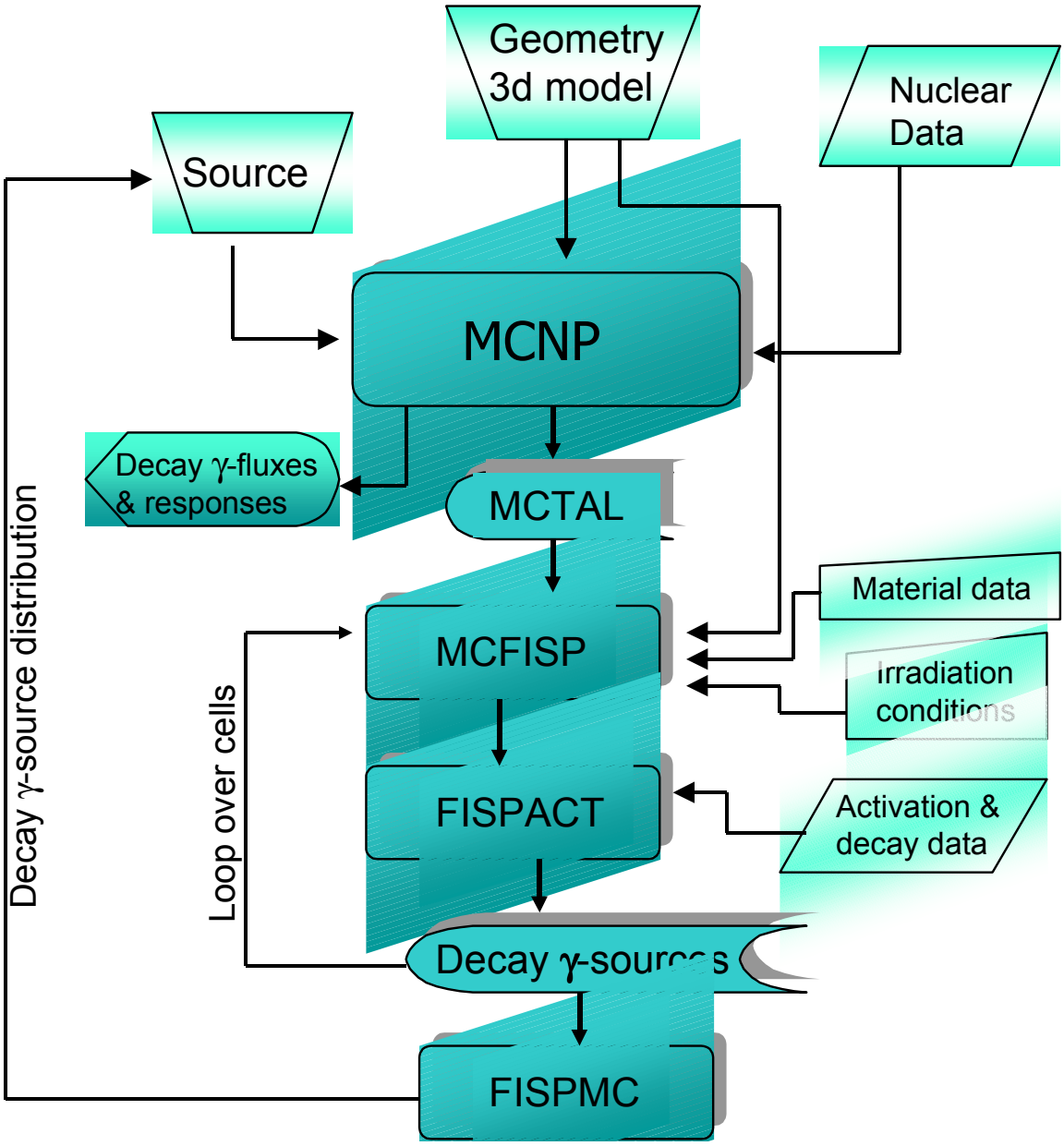

Fig. 6: Flow scheme for rigorous two step (R2S) shutdown dose rate calculations

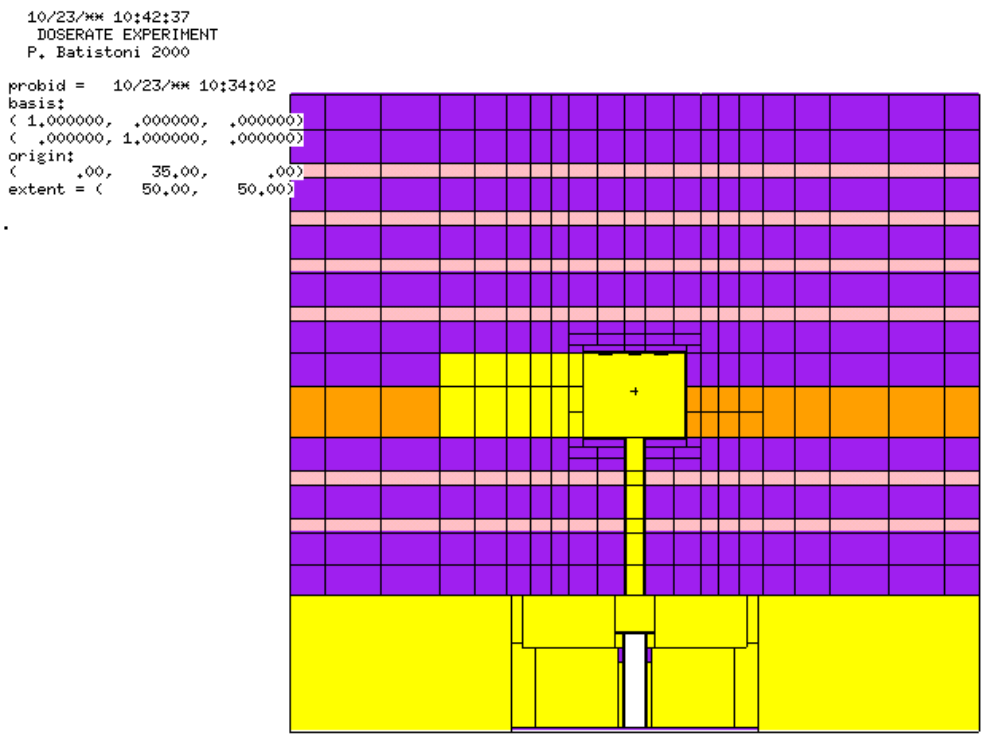

Fig. 7a: MCNP model (horizontal cut) of the mock during irradiation with no detectors and the lateral access partially closed (“irradiation model”).

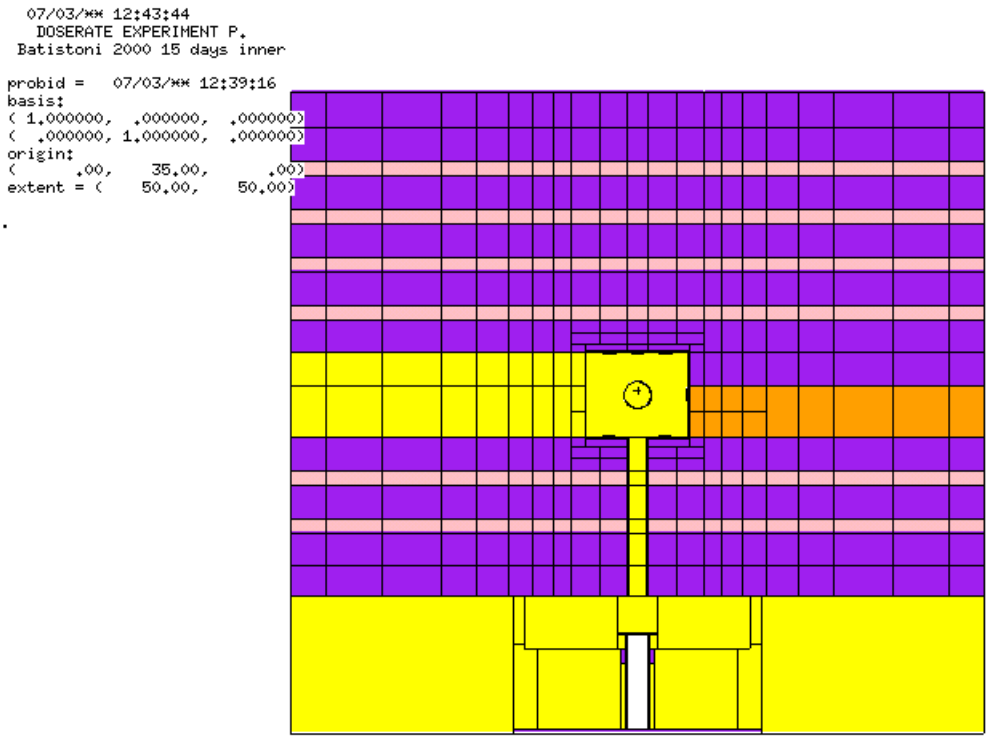

Fig. 7b: MCNP model (horizontal cut) of the mock up with G-M detector in the cavity and open lateral access used in the first irradiation campaign (“shut down model”).

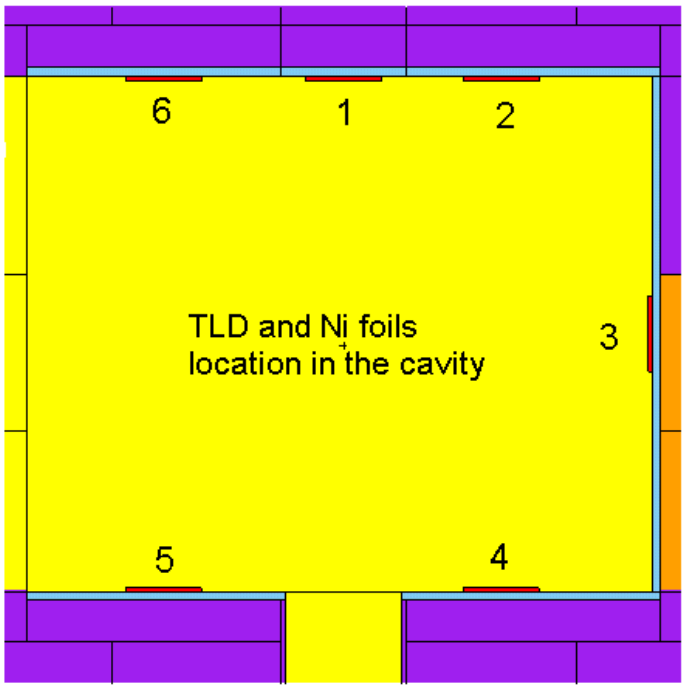

Fig. 7c: MCNP model (horizontal cut) of the mock with TLD detectors and activation foils along the cavity walls used in the first irradiation campaign ("shut down model").

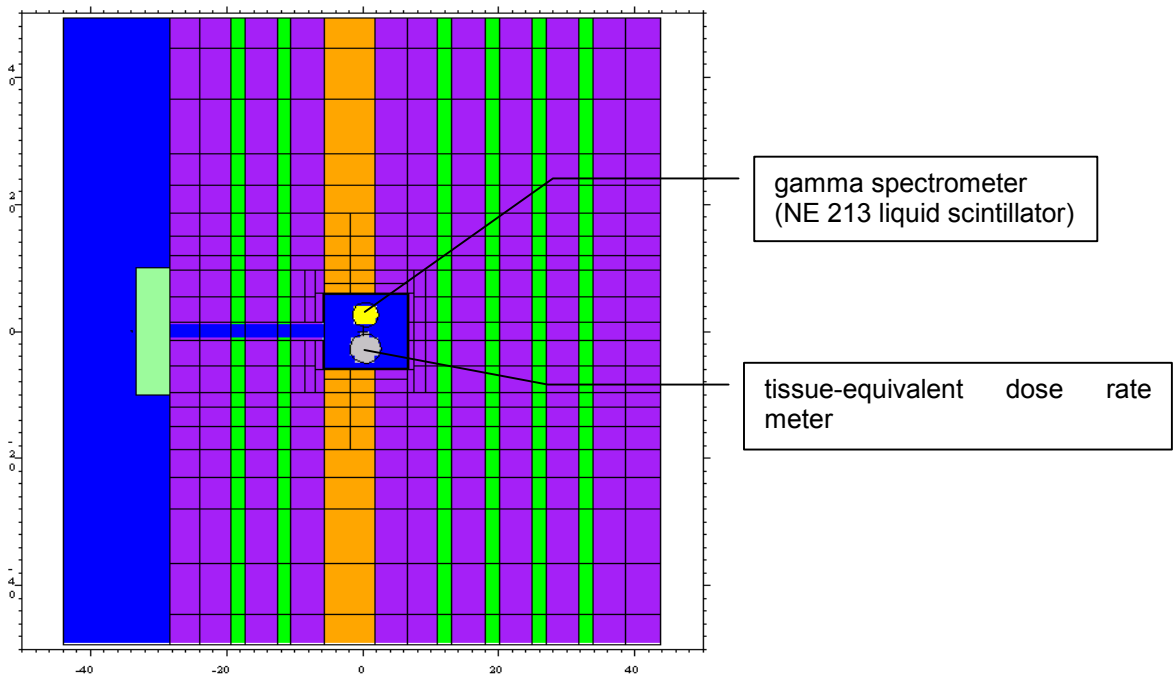

Fig. 7 d: MCNP model (vertical cut) of the mock up with dose rate and gamma spectrometers used in the second irradiation campaign ("shut down model ").

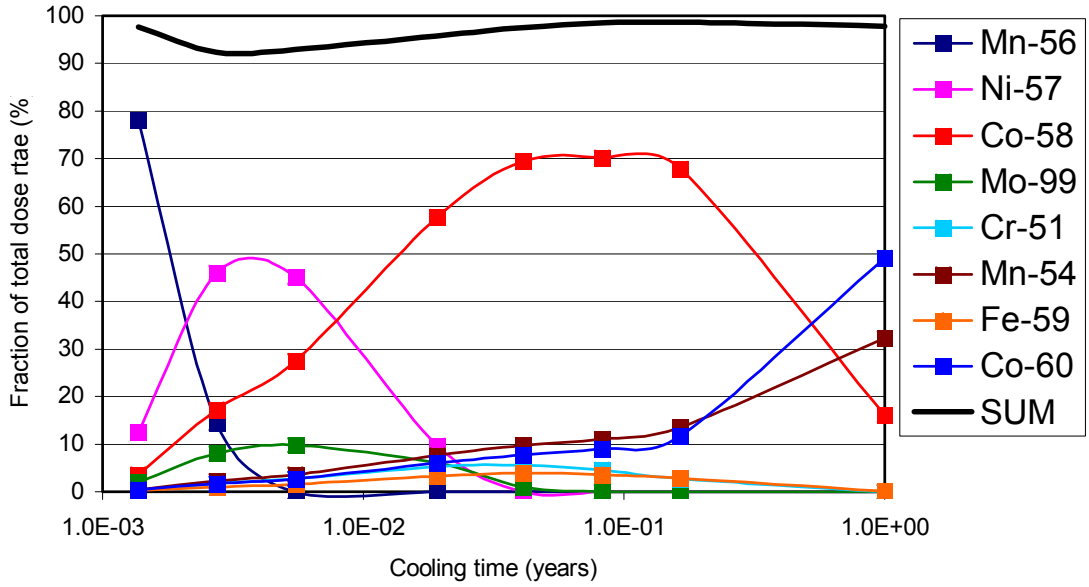

Fig.8: Contributions of most relevant radioisotopes, normalised to the total dose rate, at the cavity wall vs cooling time. The sum is given by the black line.

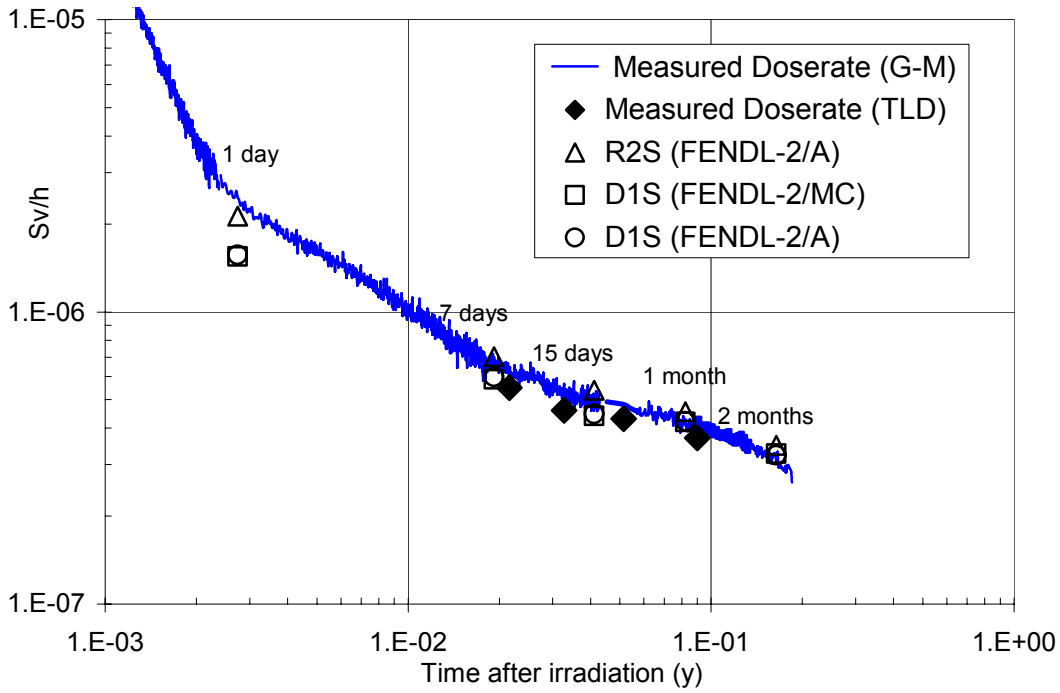

Fig. 9: Comparison between measured and calculated dose rate in the cavity centre (first experimental campaign)

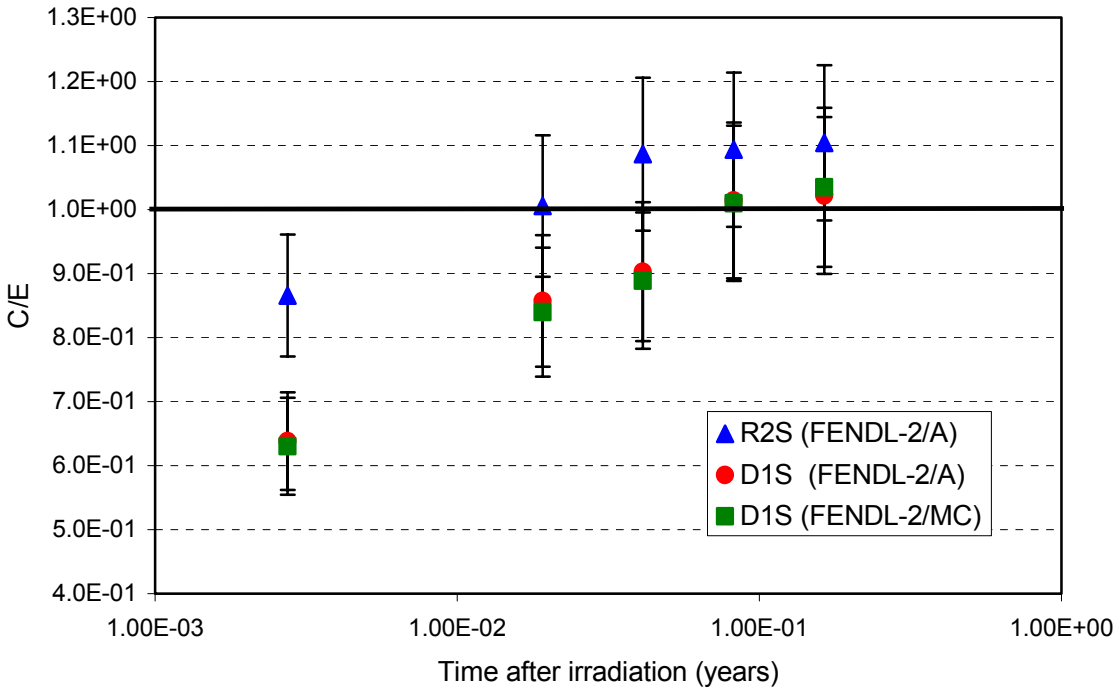

Fig. 10: C/E values for the sore rate measurements in the first experimental campaign

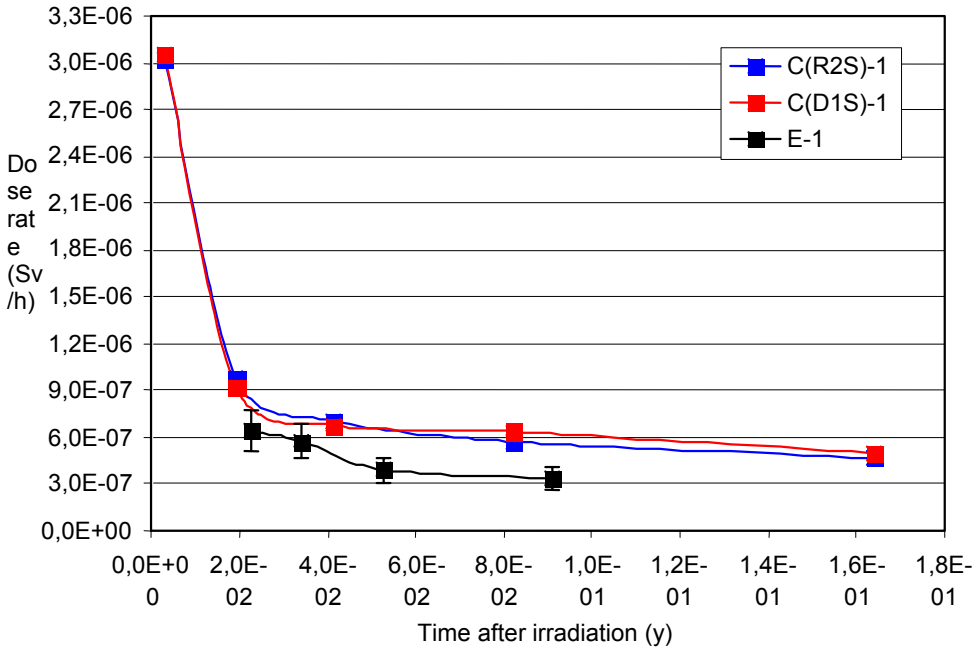

Fig. 11a: Dose rate in position1 on the cavity walls measured by TLD (black points) and calculated (color points).

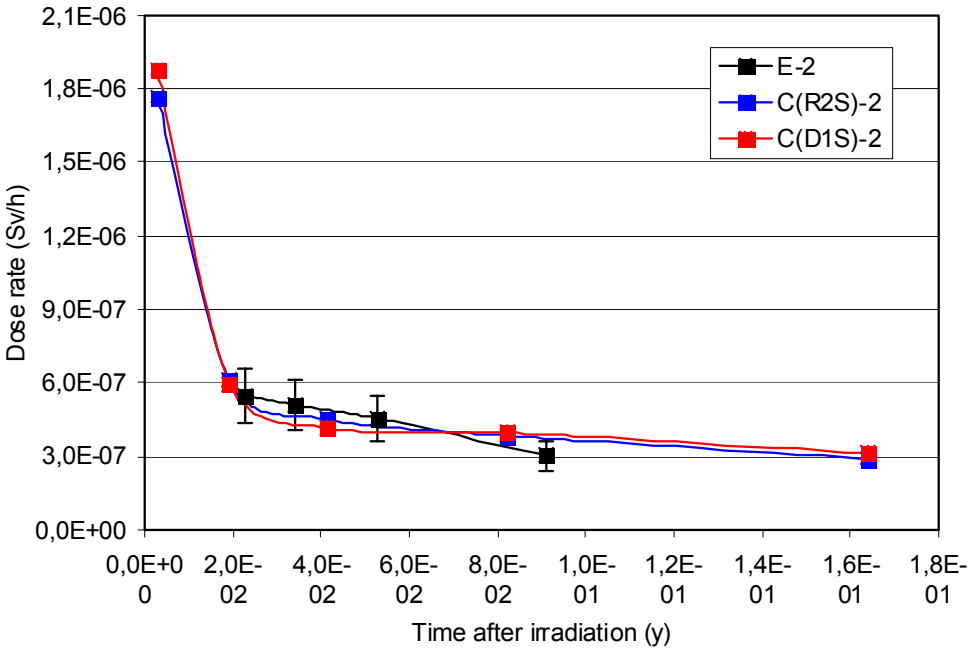

Fig. 11b: Dose rate in position 2 on the cavity walls measured by TLD (black points) and calculated (color points).

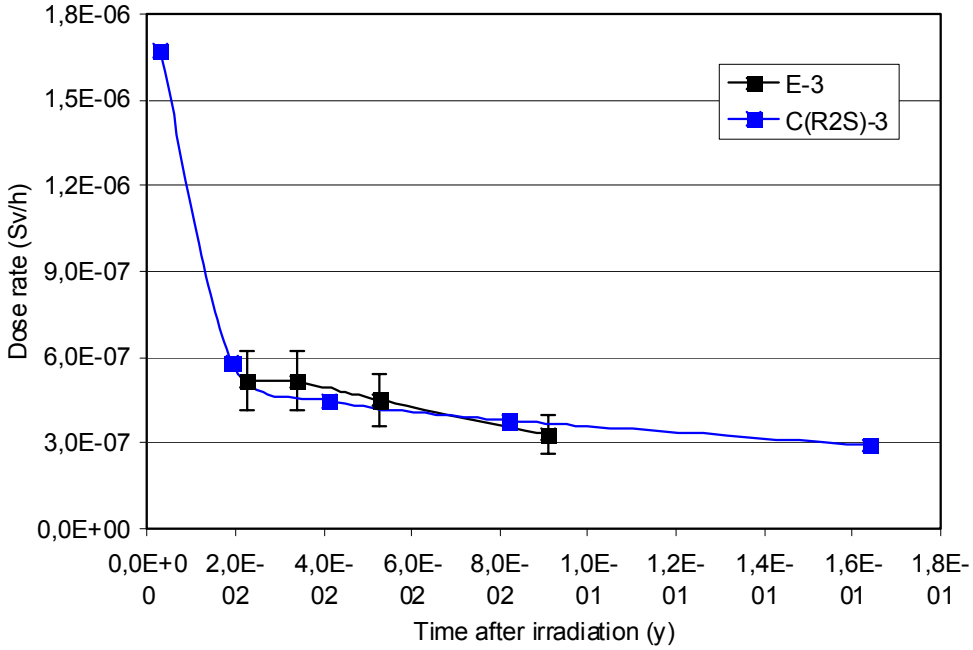

Fig. 11c Dose rate in position 3 on the cavity walls measured by TLD (black points) and calculated (color points).

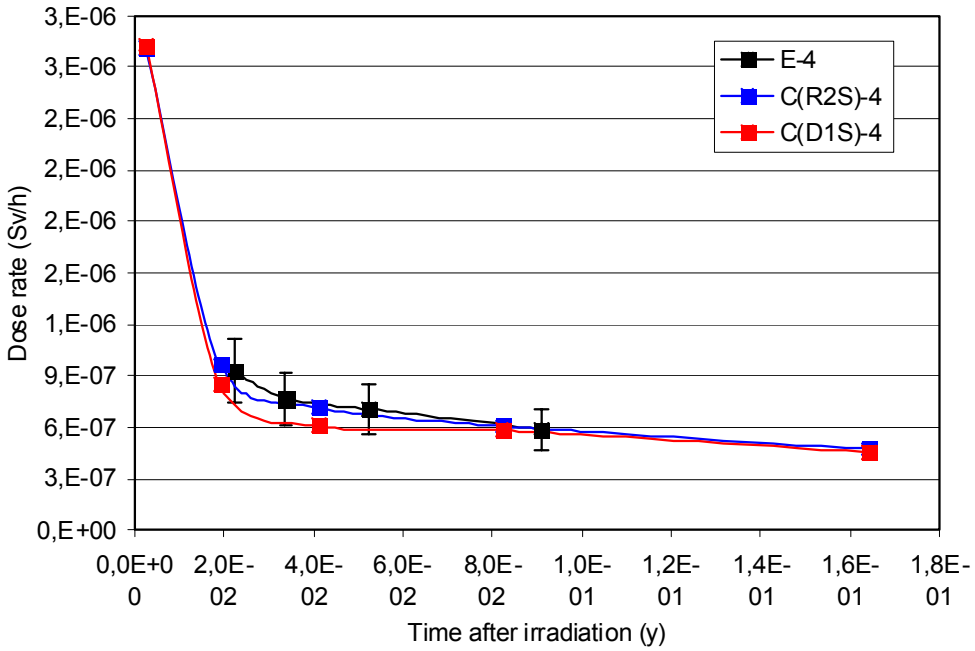

Fig.11d: Dose rate in position 4 on the cavity walls measured by TLD (black points) and calculated (color points).

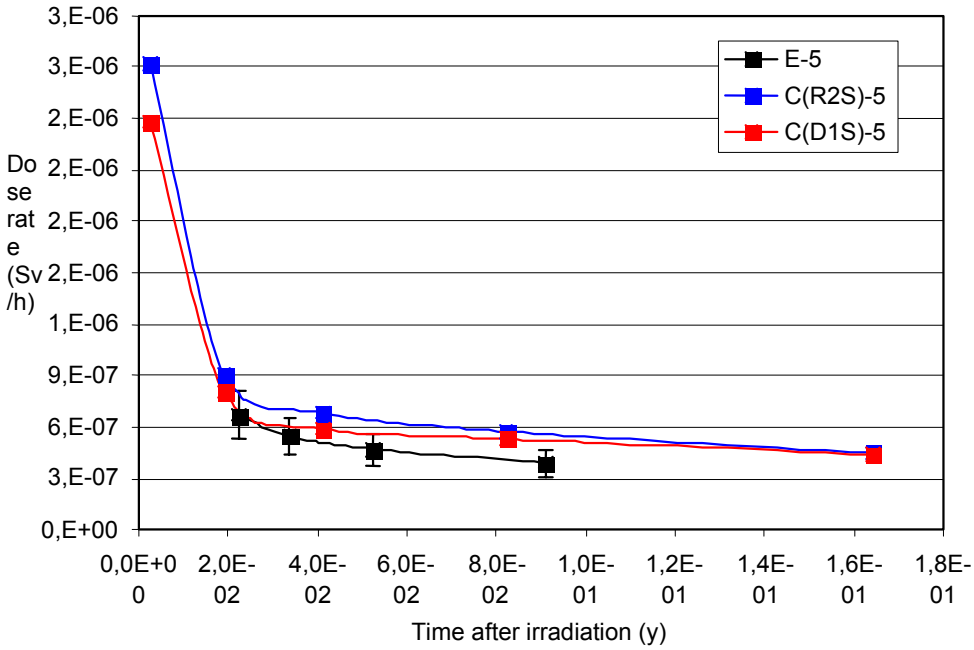

Fig. 11e: Dose rate in position 5 on the cavity walls measured by TLD (black points) and calculated (color points).

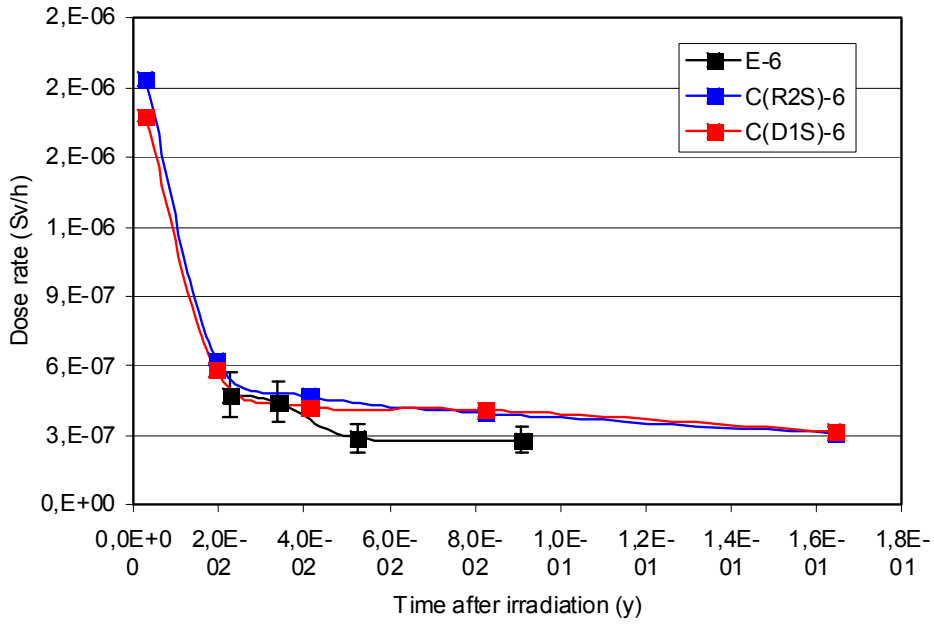

Fig. 11f: Dose rate in position 6 on the cavity walls measured by TLD (black points) and calculated (color points).

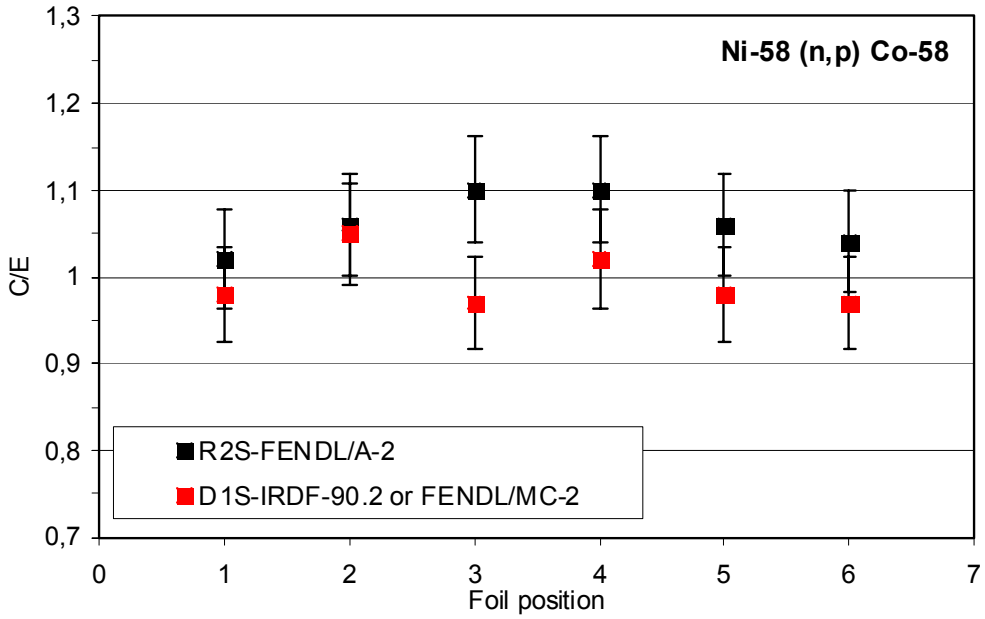

Fig.12a: C/E values for Ni-58(n,p)Co-58 activation measurements as a function of position in the cavity, obtained with R2S method (black points) and with D1S method (red points).

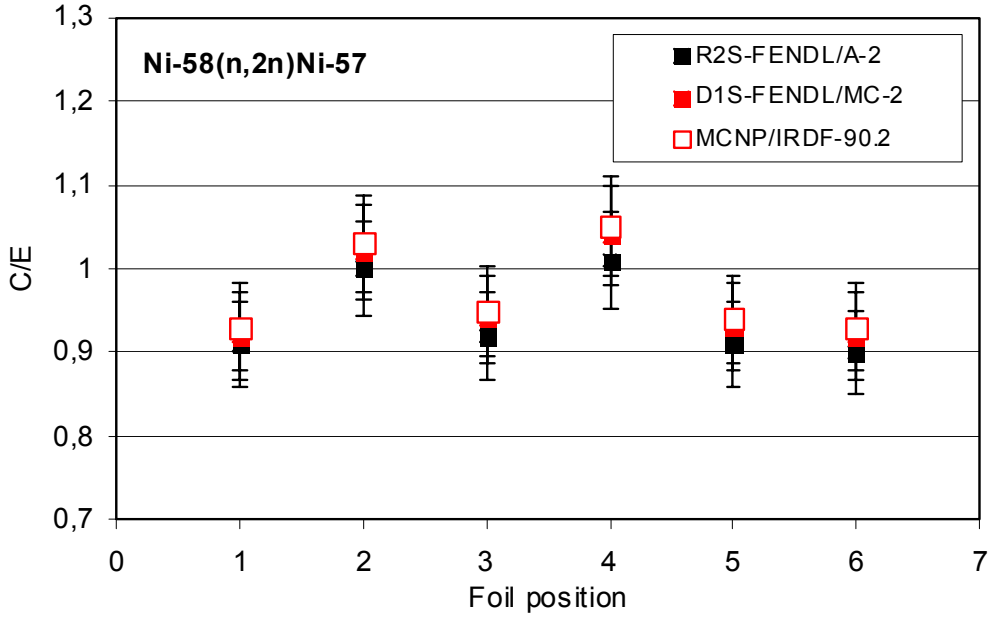

Fig.12b: C/E values for Ni-58(n,2n)Ni-57 activation measurements as a function of position in the cavity, obtained with R2S method (black points) and with D1S method using different activation cross sections (red points) for the Ni-58(n,2n) reaction.

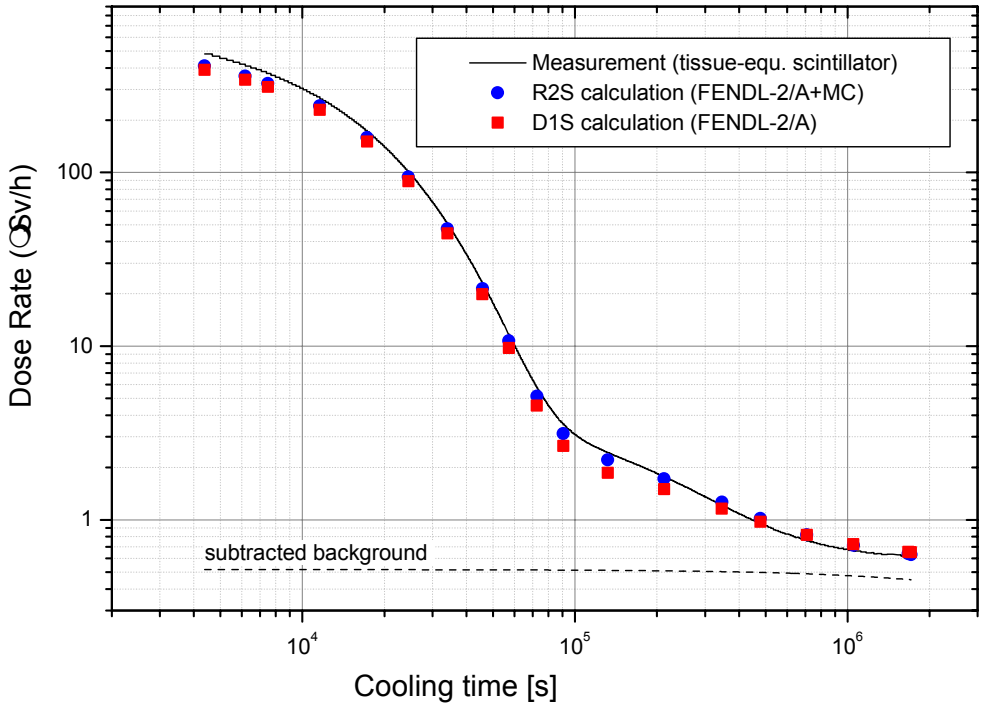

Fig. 13 a: Comparison of calculated and measured (tissue-equivalent scintillator) dose rates.

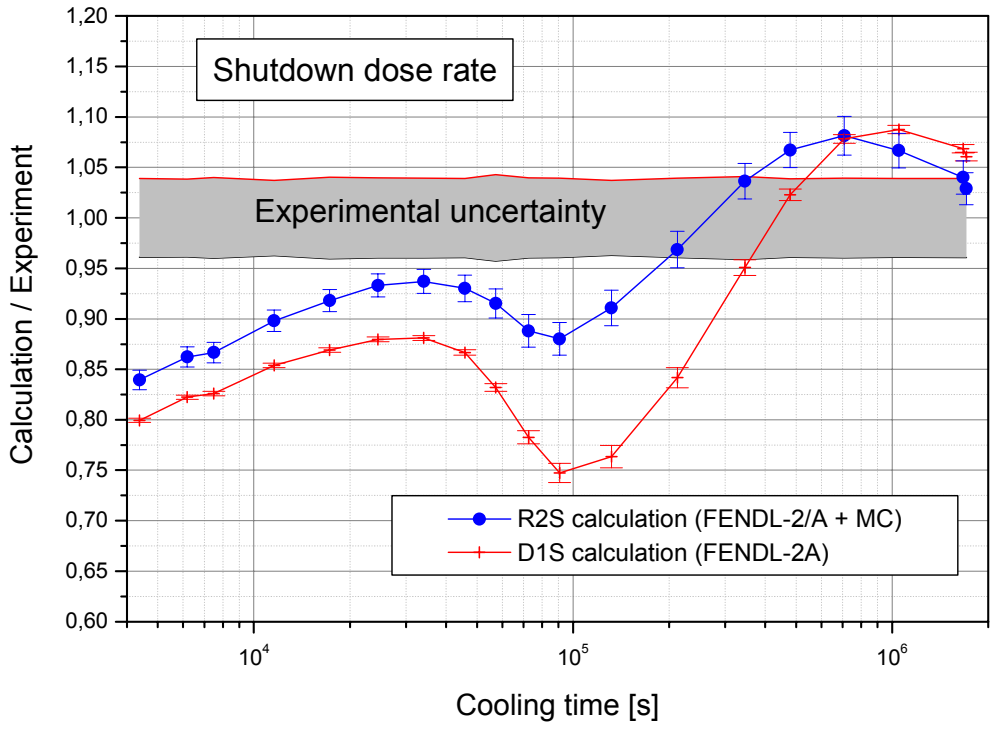

Fig. 13b: C/E (calculation/ experiment) comparison for the dose rate measured with the tissue-equivalent scintillator.

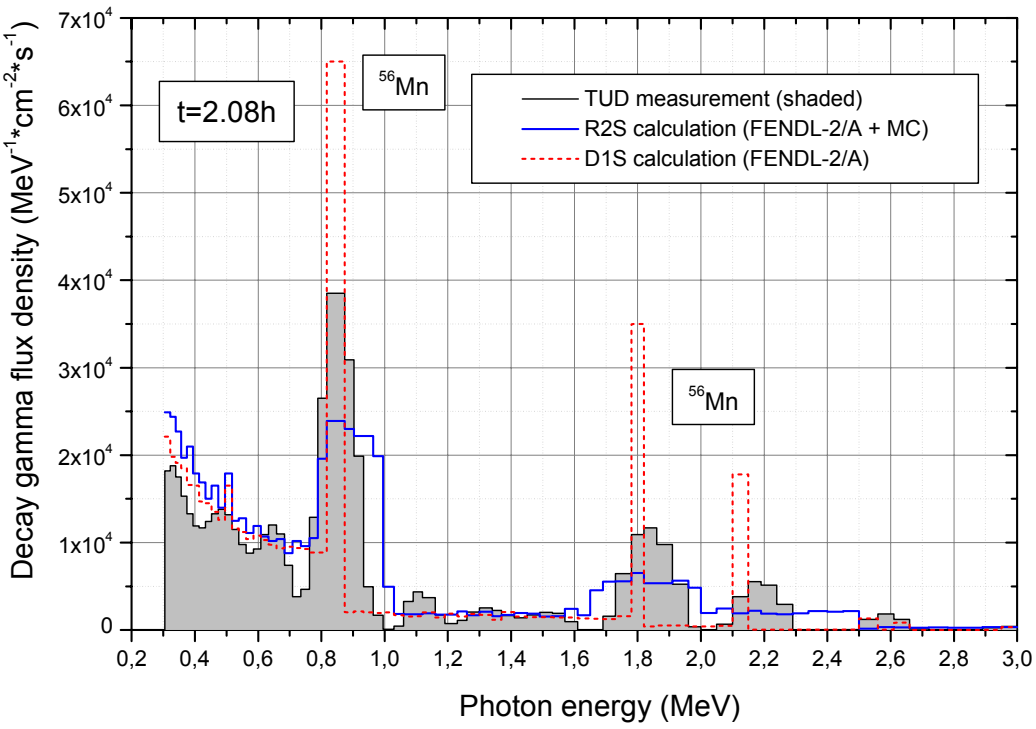

Fig. 14a: Comparison of measured and calculated decay gamma ray spectra at 2.08 h after irradiation.

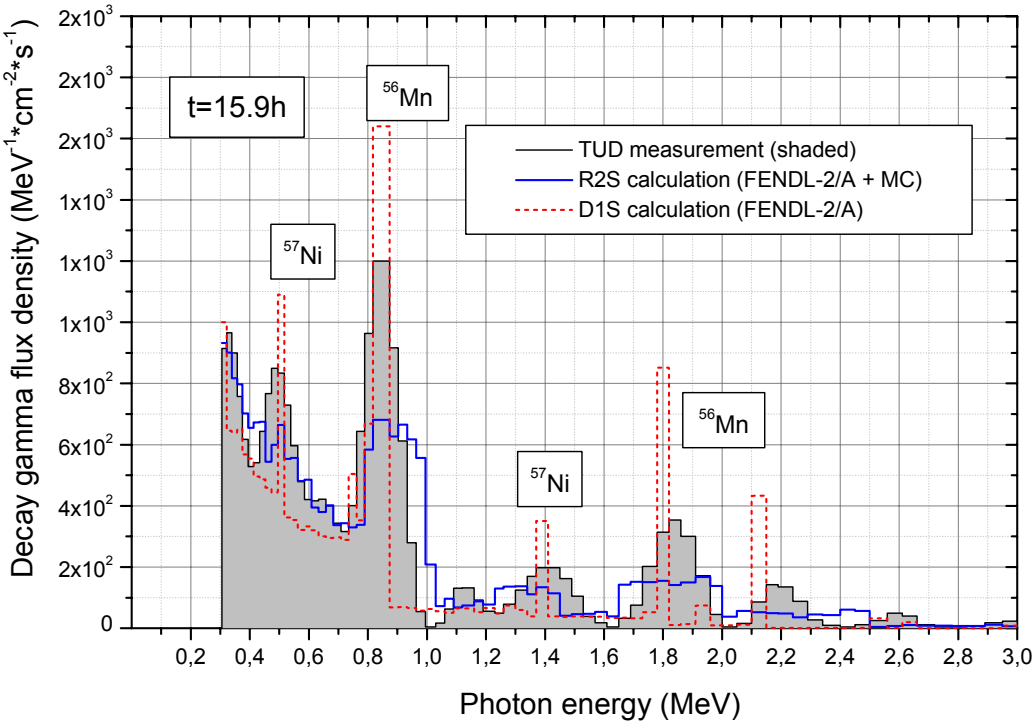

Fig. 14b: Comparison of measured and calculated decay gamma ray spectra at 15.9 h after irradiation.

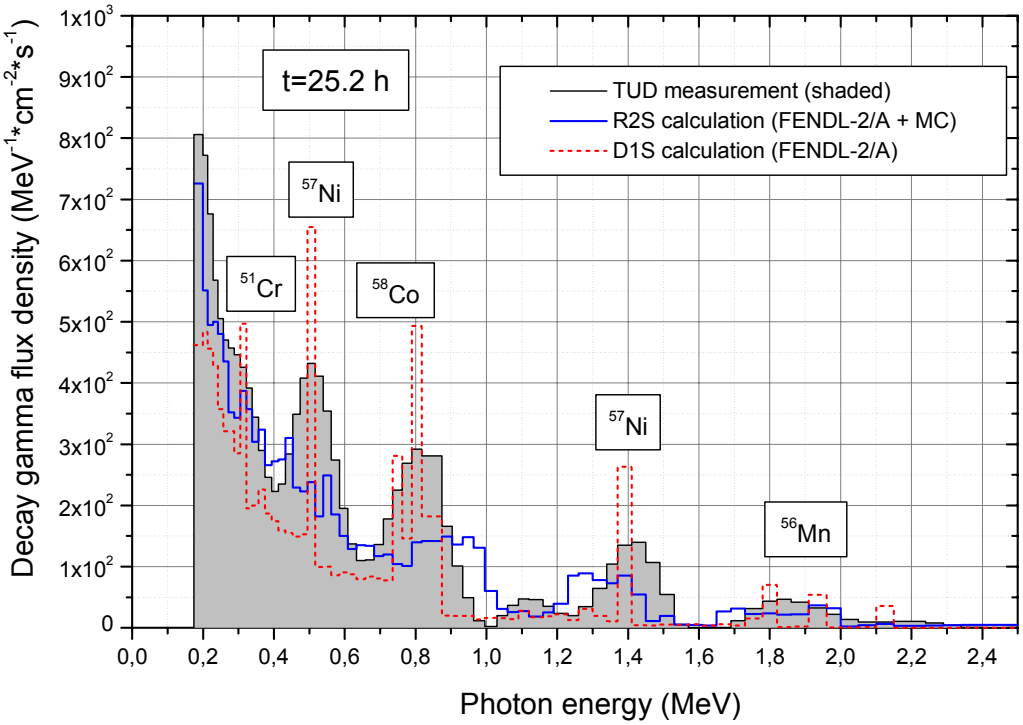

Fig. 14c: Comparison of measured and calculated decay gamma ray spectra at 25.2 h after irradiation.

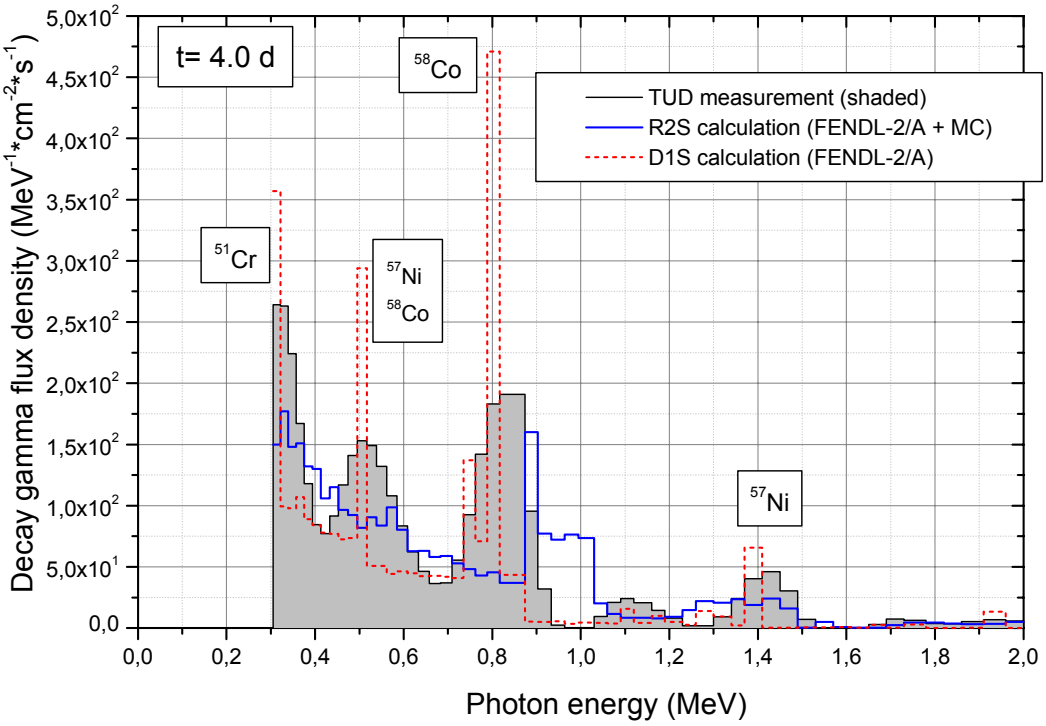

Fig. 14d: Comparison of measured and calculated decay gamma ray spectra at 4 d after irradiation

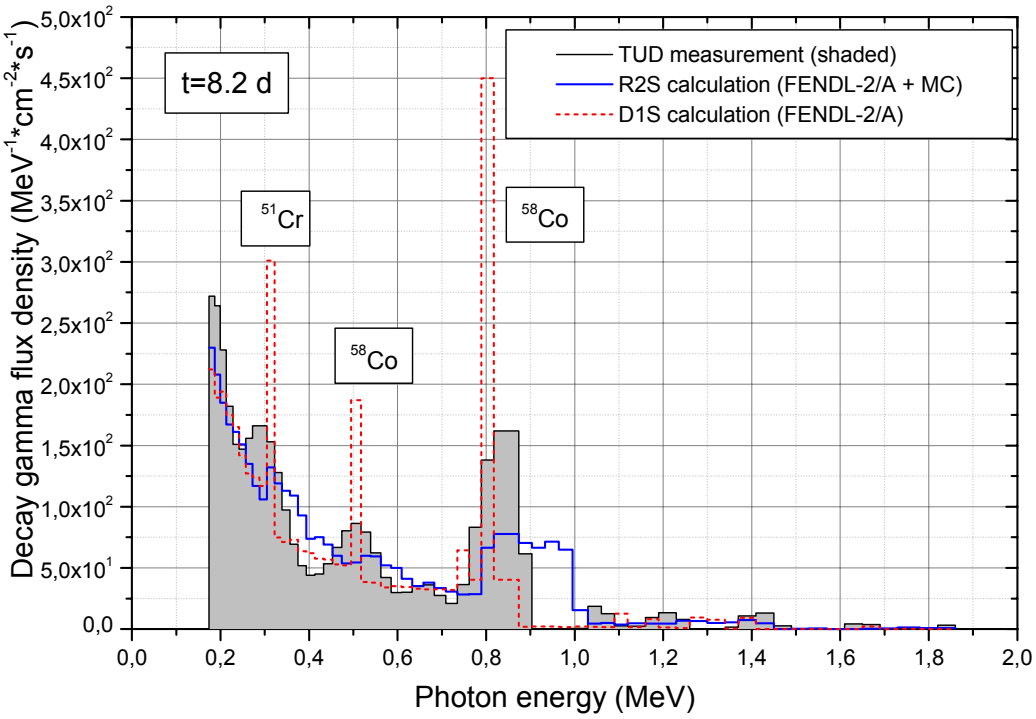

Fig. 14e: Comparison of measured and calculated decay gamma ray spectra at 8.2 d after irradiation.

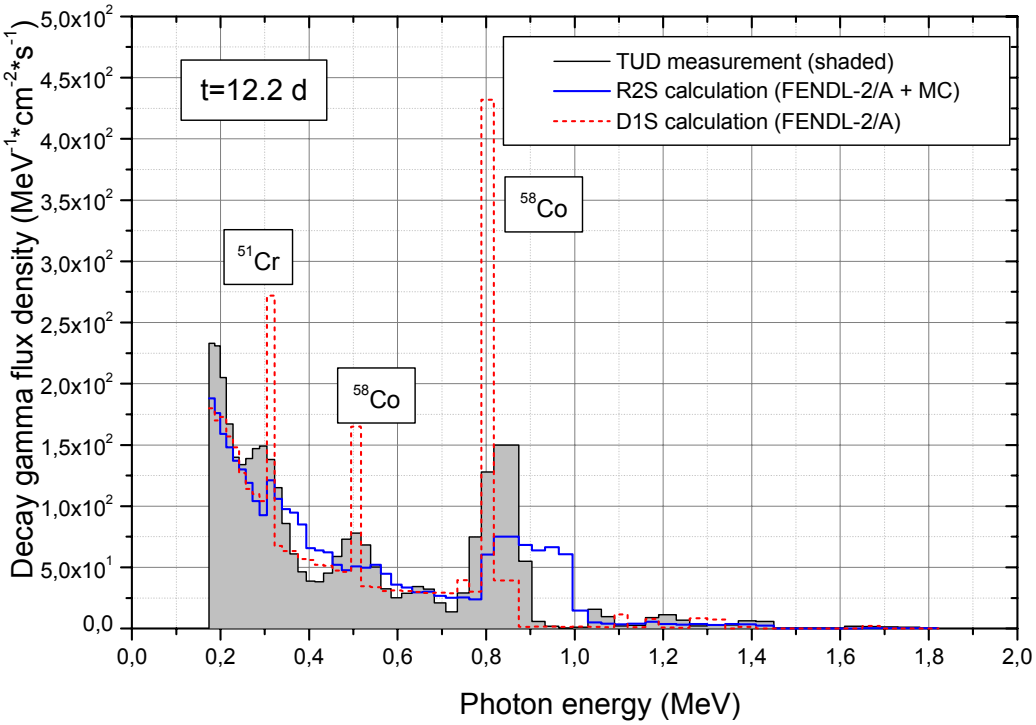

Fig. 14f: Comparison of measured and calculated decay gamma ray spectra at 12.2 d after irradiation.

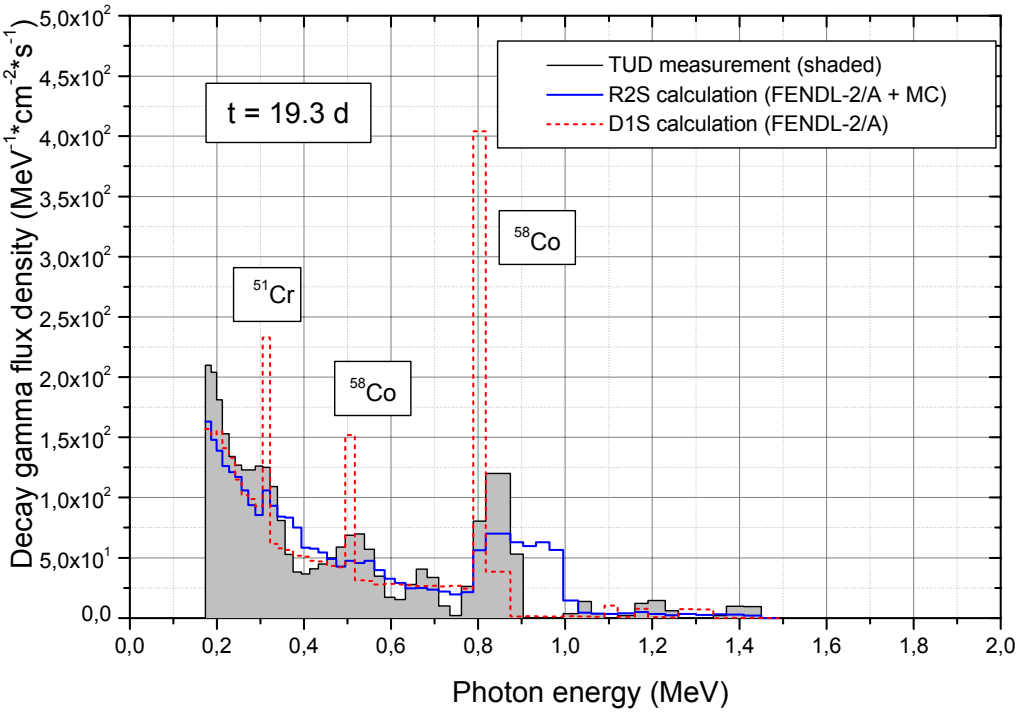

Fig. 14g: Comparison of measured and calculated decay gamma ray spectra at 19.3 d after irradiation.

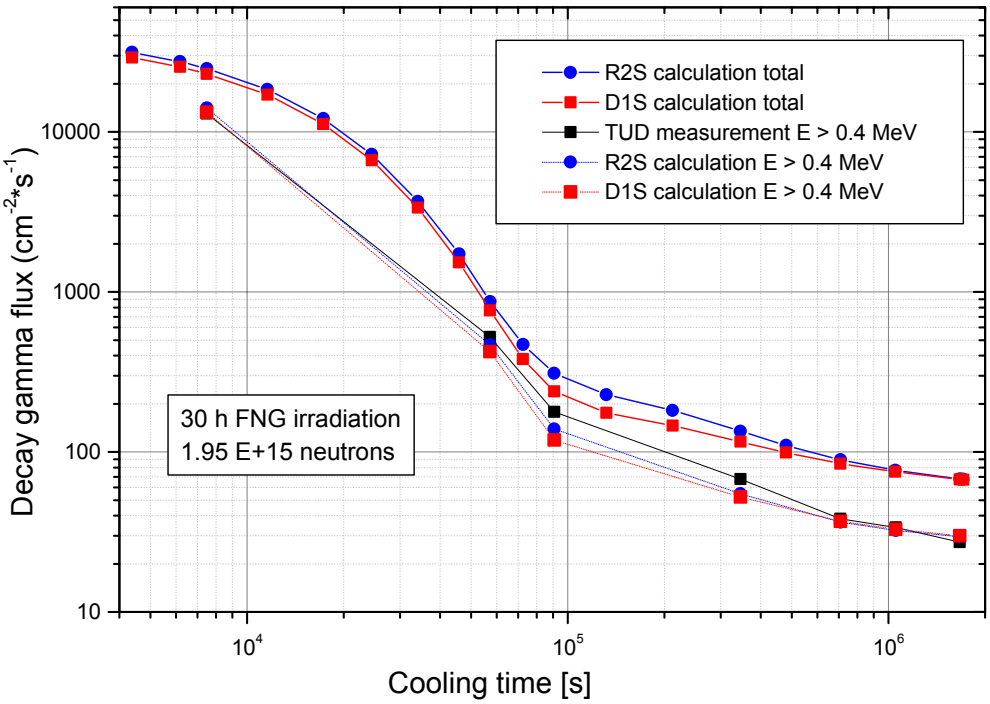

Fig. 15a: Comparison of calculated and measured decay gamma fluxes

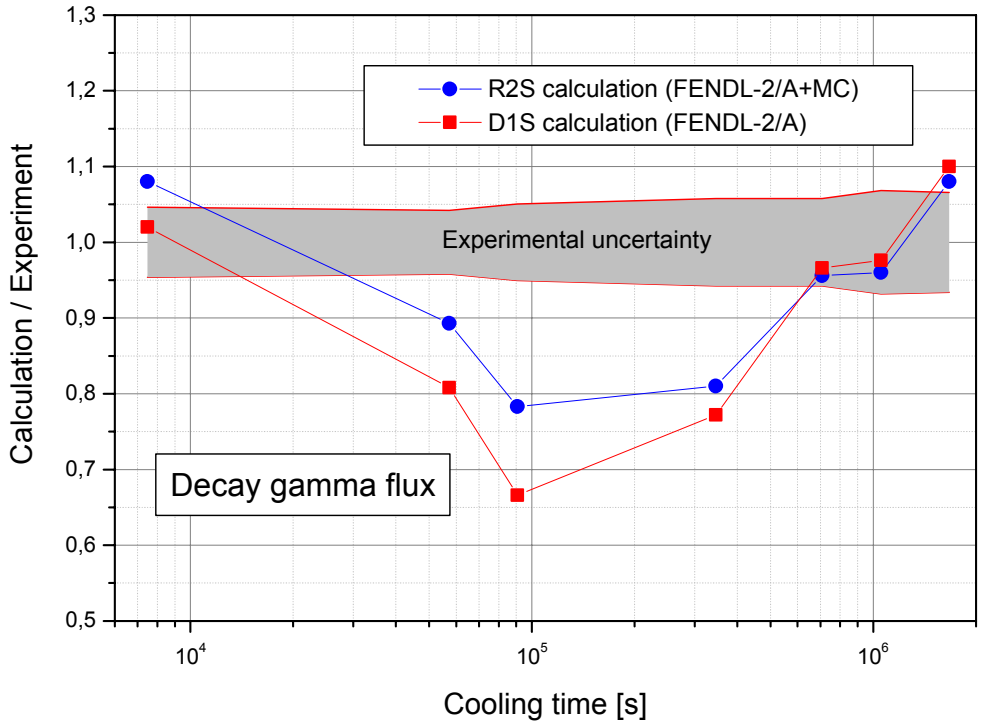

Fig. 15 b: C/E (calculation/experiment) comparison for the decay gamma ray fluxes.

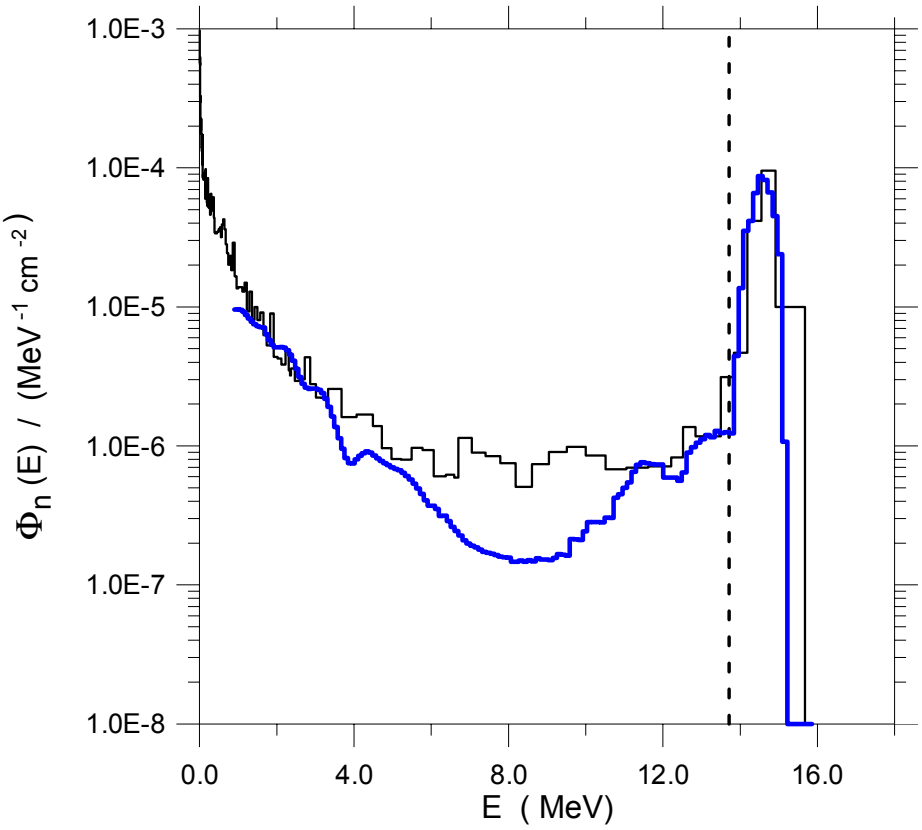

Fig. 16: Comparison of calculated (black line) and measured (blue line) neutron flux spectrum in the cavity normalised to one source neutron.